

AD-A074 096

COLUMBIA UNIV DOBBS FERRY NY HUDSON LABS

F/6 17/1

HIGH POWER SONAR TRANSMITTER USING PARALLEL INVERTER UNIT.(U)

OCT 62 F L HUNSICKER

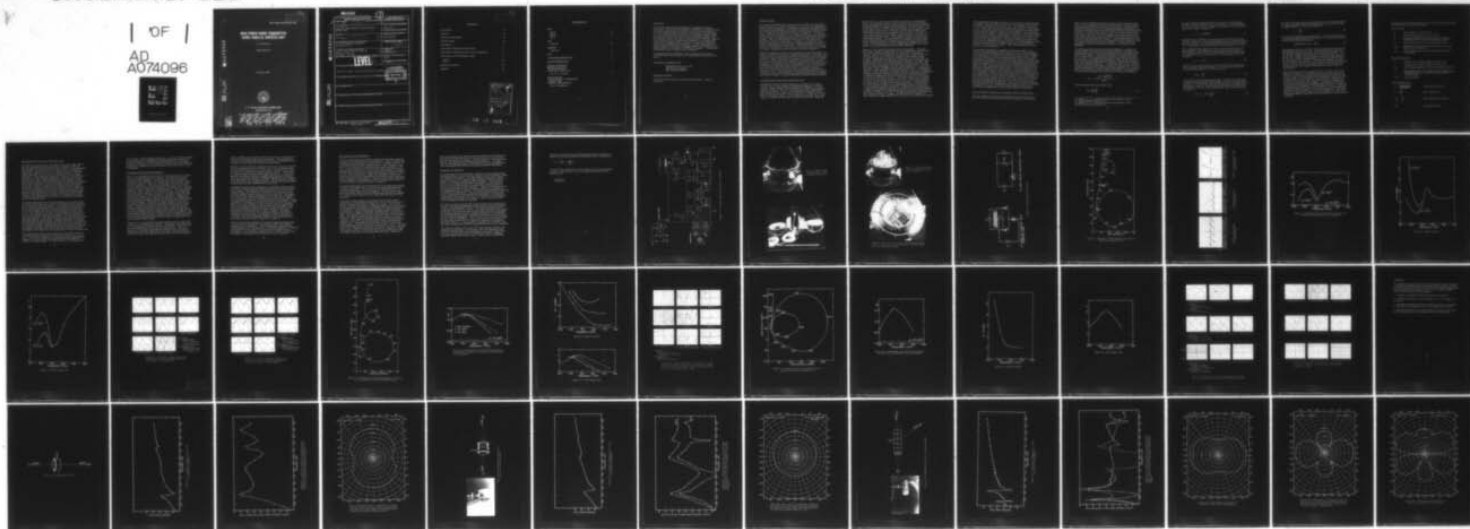
NONR-266(84)

UNCLASSIFIED

NRL-MR-1363

NL

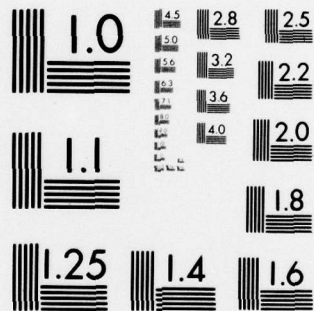
1 OF 1  
AD  
A074096



END  
DATE  
FILMED

10-79

DDC



MICROCOPY RESOLUTION TEST CHART  
NATIONAL BUREAU OF STANDARDS-1963-A

C.2  
COLUMBIA UNIVERSITY  
HUNTS-ON LABORATORY  
CONTRACT Nonr-208(04)

NRL Memorandum Report 1363

# HIGH POWER SONAR TRANSMITTER USING PARALLEL INVERTER UNIT

F. L. Hunsicker

Sound Division

5 October 1962



**U. S. NAVAL RESEARCH LABORATORY**  
Washington, D.C.

Further distribution of this report, or of an abstract,  
or reproduction thereof may be made only with the  
approval of the Director, Naval Research Laboratory,  
Washington 25, D. C. or of the activity sponsoring  
the research reported therein as appropriate.

79 09 17 044

NOV - 9 1962

DDC FILE COPY  
A074096

UNCLASSIFIED

SECURITY CLASSIFICATION OF THIS PAGE (When Data Entered)

REPORT DOCUMENTATION PAGE		READ INSTRUCTIONS BEFORE COMPLETING FORM
1. REPORT NUMBER NR-1363	2. GOVT ACCESSION NO. (18) NRL	3. RECIPIENT'S CATALOG NUMBER (9) Memorandum rept.
4. TITLE (and Subtitle) HIGH POWER SONAR TRANSMITTER USING PARALLEL INVERTER UNIT		5. TYPE OF REPORT & PERIOD COVERED Memo report
7. AUTHOR(s) Hunsicker, F. L. /Hunsicker		6. PERFORMING ORG. REPORT NUMBER
9. PERFORMING ORGANIZATION NAME AND ADDRESS U. S. Naval Research Laboratory Washington, D.C.		8. CONTRACT OR GRANT NUMBER(s) Nonr-266(84)
11. CONTROLLING OFFICE NAME AND ADDRESS Office of Naval Research, Code 220 800 North Quincy St. Arlington, VA 22217		10. PROGRAM ELEMENT, PROJECT, TASK AREA & WORK UNIT NUMBERS (12) 54P
14. MONITORING AGENCY NAME & ADDRESS (if different from Controlling Office) <b>LEVEL</b>		12. REPORT DATE 5 OCT 62
		13. NUMBER OF PAGES
		15. SECURITY CLASS. (of this report) UNCLAS
		15a. DECLASSIFICATION/DOWNGRADING SCHEDULE
16. DISTRIBUTION STATEMENT (of this report) Approved for public release; distribution unlimited.		
17. DISTRIBUTION STATEMENT (of the abstract entered in Block 20, if different from Report) SEP 20 1979		
18. SUPPLEMENTARY NOTES		
19. KEY WORDS (Continue on reverse side if necessary and identify by block number)		
20. ABSTRACT (Continue on reverse side if necessary and identify by block number)		

DD FORM 1 JAN 73 1473

EDITION OF 1 NOV 65 IS OBSOLETE  
S/N 0102-LF-014-6601

UNCLASSIFIED

172 050

SECURITY CLASSIFICATION OF THIS PAGE (When Data Entered)

AD A 074096

DDC FILE COPY



# CONTENTS

Distribution	ii
Abstract	iii
Problem Authorization	iii
Problem Status	iii
Introduction	1
Transmitter Design and Construction	1
Description of Parallel Inverter Circuit Operation	3
Performance with Transducer Loads	8
TR-34	9
R-113	11
Summary of Results	12
Appendix	14

i

Accession For	
NTIS GRA&I	<input checked="" type="checkbox"/>
DDC TAB	<input type="checkbox"/>
Unannounced	<input type="checkbox"/>
Justification	<input type="checkbox"/>
By _____	
Distribution/ _____	
Availability Codes	
Dist	Avail and/or special
A	

9 09 17 044

NOV - 9 1962

## DISTRIBUTION

### CNO

Op 32	1
Op 07	1
Op 70	1
Op 71	1

### ONR

Code 467	10
----------	----

### BUSHIPS

Code 370	1
----------	---

### NEL

2

### NAVUWTRSOUNDREFLAB

1

### NAVUWTRSOUNDLAB

1

Hudson Laboratories  
Columbia University  
145 Palisade Street  
Dobbs Ferry, New York

Dr. R. A. Frosch	2
------------------	---

Massa Division  
Cohu Electronics, Incorporated  
5 Fottler Road  
Hingham, Massachusetts

Mr. Frank Massa	1
-----------------	---

## ABSTRACT

↘ This report describes the performance of a high power sonar transmitter, which uses semiconductor components, driving 400 cycle per second electromagnetic variable reluctance type transducers. The input voltage to the transmitter is three phase, sixty cps which is first rectified and then converted to a single phase output voltage by a parallel inverter unit using silicon controlled rectifiers. By selecting the values of the series inductance and the parallel capacitor in the inverter unit so that they were resonant at the resonant frequency of the transducer load, the output voltage of the transmitter was nearly sinusoidal at this frequency. At other frequencies the output voltage was sometimes strongly distorted and changed in level due principally to the change in transducer impedance. Transmitter efficiencies of up to 75 percent were measured.

The appendix contains response curves, beam patterns and the calculated values of efficiencies of the transducer loads used in the tests. ↗

## PROBLEM AUTHORIZATION

BUSHIPS SF 001-03-03-8134  
ONR 001-03-44-4062  
NRL Problem 55S02-10

## PROBLEM STATUS

This is an interim report on one phase of the project. Work is continuing.



## INTRODUCTION

The merits of semiconductor circuits are well known and those that are of chief interest for a sonar transmitter are: mechanical ruggedness, freedom from microphonics, instantaneous operation and high efficiency. The transmitter described in this report is basically a parallel inverter circuit using silicon controlled rectifiers with additional circuitry to make it suitable to be used to drive a sonar transducer. All the semiconductors in the transmitter circuit operate in a switching mode which by itself makes for efficient operation and thus simplifies the cooling problem. Also, the performance of the circuit is not appreciably affected by changes of temperature, changes in current levels or unwanted feedback which can in the case of high gain amplifiers cause a change in performance or instability. Silicon controlled rectifiers are preferred to transistors in the inverter unit because they are available with larger voltage and current ratings and are less expensive.

Because the parallel inverter circuit operates in a switching mode, its analysis is difficult even for the simplest type of load. Its output is not sinusoidal but in special cases may be close enough so that for practical purposes it may be considered as a generator of a sine wave of voltage or current. With a load of the complexity of a transducer, an exact analysis of the inverter circuit and load becomes too cumbersome to be worthwhile. Laboratory tests of the transmitter with a resistive load provided some information about performance but were not felt sufficient to establish the worth of the circuit as a sonar transmitter. Therefore, tests of the transmitter with a transducer load were performed at the U. S. Navy Electronics Laboratory Pend Oreille Calibration Station, where its performance could be established and compared with the performance of a linear amplifier driving the same transducer.

## TRANSMITTER DESIGN AND CONSTRUCTION

The parallel inverter circuit's function is to convert the dc input voltage to an ac output voltage of controllable frequency. Such circuits are usually operated from regulated, well-filtered dc voltage supplies. However, they can also be operated from dc generators or multi-phase rectifier circuits. It was decided to design the transmitter to operate from three-phase, 440 volt ac, because of the availability of this type of power. In the transmitter this 440 volt ac input voltage is stepped down and then rectified to provide the voltage for

the inverter unit. For a given load the only means to control output power is by changing the input voltage so that for the test of the transmitter the output was controlled by using a three-phase autotransformer to adjust the input ac voltage to the transmitter. In order to start, and more important to be able to stop, the inversion process a gate circuit using a high current silicon controlled rectifier was included in the transmitter which serves as a gate for the dc current. This gate circuit is also used as a circuit breaker to interrupt the dc current if a current fault develops which, if not stopped, results in the loss of the controlled rectifiers. The transmitter was designed to be controlled from a remote location so that entering it are low level pulses which control the output frequency and the starting and stopping of the transmitter. The transmitter can deliver 2000 watts of power into a unity power factor load at frequencies from 300 to 4000 cps.

Figure 1 is the complete schematic for the transmitter. The three-phase input voltage is stepped down by three single phase transformers each with a 480 volt primary and a 25 volt and 44 volt secondary winding. The 44 volt secondaries are connected in a delta and the 25 volt secondaries in a wye and each supplies a three-phase bridge rectifier. The bridge rectifiers are connected in series and, due to the phase difference of the delta and wye connections, the output ripple frequency of the sum of the bridge rectifier voltages is 720 cps. The positive side of the rectifier goes directly to the inverter unit consisting of an output transformer (12 ohms center tapped to 62.5, 150, 200, 250 ohms), a pair of 2N688 silicon controlled rectifiers, a commutation capacitor across the output transformer primary, and a 1.6 millihenry inductor. An RC network is in parallel with each of the silicon controlled rectifiers and an RL network in series with the commutation capacitor to suppress voltage and current transients due to the switching action of the silicon controlled rectifiers. After the inverter unit is a gating circuit for the dc current which uses a 2N1913. When this controlled rectifier is in the off state it has across it all the dc voltage and only a few milliamperes leakage current can flow through it. A signal pulse to its gate turns it on and the dc voltage appears across the inverter circuit starting the inversion process. To stop the inversion process, a signal pulse is applied to the gate of the 2N1774, low current controlled rectifier, turning it on and placing the negative capacitor voltage across the 2N1913, turning it off. The dc voltage is again across the 2N1913 and the inversion process is stopped. The 200 microfarad capacitor is kept charged by voltage coming from one of the 44 volt secondary windings.



Also supplied by the bridge rectifier is a 15 volt zener diode regulated dc supply for the flip-flop circuit which drives the gates of the silicon controlled rectifiers in the inverter unit. The flip-flop is driven by low level pulses from a unijunction relaxation oscillator in the control circuit. The output from the two sides of the flip-flop is differentiated and transformer coupled to the gates of the 2N688's. Also operating from the 15 volt supply is a peak current sensing circuit which produces a pulse if the dc current instantaneously rises above a set level. This circuit senses the voltage due to the dc current across a 0.009 ohm shunt in series with the 2N1913. When this voltage rises above 250 millivolts, the 1N2940 tunnel diode switches to its high impedance state generating a pulse which is amplified and fed into the gate of the 2N1774. The 2N1774 then conducts, which turns off the 2N1913 and stops the inversion process.

The physical positioning of components in the transmitter is not critical to the performance of the various circuits. The transmitter on which the tests were made was installed in a steel vessel designed to be submerged to a depth of several thousand feet in water. Figure 2 shows an exterior view of the stainless steel vessel in which the transmitter is contained. The vessel with the transmitter weighs 700 pounds and has been tested at an external hydrostatic pressure of 1500 pounds per square inch. It consists of two hemispherical end domes (figure 3) 18 inches in diameter which are bolted to the flanges of the eight-inch-long cylindrical center section. All the transmitter components are mounted to the center section so that both domes can be removed to gain access to the transmitter. Large components, such as transformers, inductors and tuning capacitors, are mounted on two plates (figure 4) which are bolted to the inner surface of the flanges on the center section. Figure 5 shows an interior view of the center section with one of the plates removed. The inner surface of the flange has been machined smooth and is used as a heat sink for the stud-mounted semiconductor components. There are four cables entering the center section: one bringing the three-phase ac power, one for the single-phase ac output, one for the control signals, and the last is available for bringing out a monitor signal from the transmitter.

#### DESCRIPTION OF PARALLEL INVERTER CIRCUIT OPERATION

The basic parallel inverter circuit (figure 6a) has two like states in which one of the silicon controlled rectifiers conducts current with

about a one volt forward drop while the other blocks current and has across it the transformer primary voltage minus the forward voltage drop of the controlled rectifier which is conducting. Switching back and forth between states is accomplished by applying signal pulses of the desired frequency alternately to the gate terminals of the controlled rectifiers. A steady state analysis of the circuit requires matching of the final values of current and voltages of one state with the initial values of the next state. Such an analysis has been published for the case when the load is purely resistive.<sup>1</sup> A later paper gives an analysis for a load consisting of a resistance and a series inductance under the condition that the dc current is constant.<sup>2</sup> These are the only quantitative analyses of the parallel inverter circuit known to be published.

To obtain a qualitative picture of inverter operation, consider the inverter (figure 6a) and its half period equivalent circuit (figure 6b) during which one of the silicon controlled rectifiers conducts current and the other blocks. The initial conditions for the half period are that a current flows in the inductor and there is voltage on the capacitor as shown. The voltage on the capacitor starts to reverse due to the action of the dc supply and the duration of time between the beginning of the half period and when the capacitor voltage goes through zero is the commutation time  $t_c$ . During this time,  $t_c$ , the controlled rectifier which was conducting in the previous half period is reverse biased and regains its forward current blocking ability if  $t_c$  is greater than its turn-off time of about twenty microseconds. The solution to the current and voltages in the inverter circuit will be functions of

$$\exp - \frac{1 \pm \sqrt{1 - 16R^2 C_c / L}}{8RC_c} t$$

These solutions will be oscillatory when

$$R > \frac{1}{4} \sqrt{\frac{L}{C_c}} \quad (1)$$

- 
1. Wagner, C. F., "Parallel Inverter with Resistive Load", Electrical Engineering, Nov 1935
  2. Wagner, C. F., "Parallel Inverter with Inductive Load", Electrical Engineering, Sep 1936

To obtain a nearly sinusoidal output, the natural oscillation period should be made the same as the inverter period  $T$ . If the damping of the circuit is small,  $8RC_c$  is equal to a half period or more; then the output will be nearly sinusoidal if

$$T \simeq 2\pi \sqrt{4LC_c} \quad (2)$$

Satisfying these conditions is not necessary for the operation of the inverter. However, it was found that when they were satisfied the output of the inverter was a good approximation to a sinewave and sufficient commutation time was provided for the operation of the inverter.

For a given load the output power of the inverter depends on the dc input voltage  $\bar{V}$ . The efficiency of conversion of dc to ac power,  $\eta$ , for a parallel inverter circuit has been found to be 80 to 90 percent for frequencies up to several kilocycles. The output power can be written as

$$P = \eta \bar{V} \bar{I} \quad (3)$$

Where  $\bar{V}$  is the dc input voltage to the inverter and  $\bar{I}$  is the average value of current from the dc supply. It is convenient to define an equivalent input resistance for the inverter as

$$R_{in} = \frac{\bar{V}}{\bar{I}} \quad (4)$$

which will be found by measuring  $\bar{V}$  and  $\bar{I}$ . During a half period the current from the dc supply flows through only one of the controlled rectifiers. Its waveform is intermediate between a rectangular pulse and half of a sinewave. Assuming the more severe waveform, the half sinewave, the rms current through one of the silicon controlled rectifier is

$$\frac{\pi}{4} \bar{I} = 0.78 \frac{\bar{V}}{R_{in}} \quad (5)$$



Due to the oscillatory nature of the inverter circuit, the peak voltage  $V_P$  appearing on the silicon controlled rectifier is several times the dc supply voltage  $\bar{V}$ . This ratio is defined as

$$k = \frac{V_P}{\bar{V}} \quad (6)$$

which will be called the peak voltage ratio. The last quantity useful in defining the performance of the inverter is the ratio of commutation time to the inverter period; that is,

$$\text{commutation ratio} = \frac{t_c}{T} \quad (7)$$

The quantities (4), (6), (7) define the most important features of the performance of the inverter unit. The input resistance determines the required current rating of the silicon controlled rectifier,  $I_{rms}$ , and the peak voltage ratio determines the voltage rating,  $V_{bo}$ , in terms of  $\bar{V}$ . Together they determine the maximum output power of the inverter circuit by expression (3). It is also necessary to know the commutation ratio and how it changes with frequency and load because, when it falls below a value to provide sufficient commutation time to allow the silicon controlled rectifier to turn off, both controlled rectifiers will conduct at the same time which results in a current fault.

When the parallel inverter circuit is used in a system, such as the transmitter in figure 1, its performance is even more difficult to analyze. It will be seen from the test results that the input voltage to the inverter circuit produced by the transformer connections and bridge rectifier is not a constant. Its waveform is affected by the inverter circuit and its load. Therefore,  $\bar{V}$  will be redefined to be the average value of the input voltage. A transducer load for the inverter circuit may have a high Q and large capacitive or inductive components to its impedance. The condition on L and C<sub>c</sub> to obtain a sinusoidal output will be found using as the value of R the reflected impedance of the transducer at its resonant frequency. If the transducer at resonance has a large reactive component, this should be balanced by adding an appropriate reactive element in series with the transducer.

The definitions of the symbols of the circuit values and other quantities in the inverter circuit are listed below.

#### Circuit Values

$L$	Series inductor in inverter unit
$C_c$	Commutation capacitor in inverter unit
$R$	Reflected impedance of load on secondary of output transformer across one of the primary windings
$C_T$	Tuning capacitor in series with transducer load
$I_{rms}$	RMS forward current rating of the silicon controlled rectifier in inverter unit
$V_{bo}$	Peak voltage rating of silicon controlled rectifier in inverter unit

#### Measured Quantities

$\bar{V}$	Average value of input voltage to inverter unit
$\bar{I}$	Average value of input current to inverter unit
$V_p$	Peak voltage appearing on silicon controlled rectifiers
$t_c$	Commutation time - the length of time during the inversion period which the silicon controlled rectifier is reversed biased
$T = \frac{1}{f}$	Inversion period

#### Calculated Quantities

$\eta = \frac{\text{output power}}{\text{input power}}$	Transmitter efficiency
$k = \frac{V_p}{\bar{V}}$	Peak voltage ratio
$R_{in} = \frac{\bar{V}}{\bar{I}}$	Input resistance of inverter
$\frac{t_c}{T}$	Commutation ratio



## PERFORMANCE WITH TRANSDUCER LOADS

The tests of the transmitter, which were performed in May 1962 at the NEL Pend Oreille Calibration Station, involved two 400 cps electromagnetic variable reluctance type transducers with permanent magnet bias: Massa Division of Cohu Electronics, Incorporated, transducers, type TR-34 and R-113. Also available for use with these transducers were cylindrical baffles and pressure release assemblies. The transducers were first driven by a sinusoidal voltage from a vacuum tube linear amplifier. With the input current held constant, input voltage and power were measured at various frequencies in order to determine the electrical impedance characteristics of the transducers. Acoustic pressure levels and beam patterns were recorded to determine the acoustic efficiency of the transducer. Response curves taken at constant current, beam patterns, and the calculated value of efficiency for the transducer are included as an appendix in this report. Beam patterns and acoustic pressure levels at resonance were also taken at the same current levels with the experimental transmitter. The performance of the transducer was the same with both the linear amplifier and experimental transmitter drive.

It had been expected that one of the transducers with a baffle would be capable of accepting two kilowatts of input power which would be the full capacity of the transmitter. It was found from the tests with the vacuum tube amplifier drive that the transducers could not be driven at more than 300 watts input without producing distortion in the acoustic radiation for the TR-34 or closing the air gaps in the R-113. The transmitter was thus limited to operating at less than a sixth of its full output capacity which meant it was not operating at maximum efficiency. The measured efficiency of conversion of three-phase input power to single-phase output was from 60 to 75 percent depending upon the input voltage. An appreciable part of the losses were from the forward voltage drops in the four silicon rectifiers and two controlled rectifiers through which the dc current must flow. At full operating voltage, losses due to the forward drops are a smaller percentage of the total losses so that the overall efficiency of the transmitter at full capacity can be expected to be from 75 to 80 percent.

The performance of the inverter circuit was of primary concern in the tests and this is reported in terms of the values of  $R_{in}$ ,  $k$ , and  $t/T$ . To drive the transducer at a constant current while changing frequency, it was necessary to change the input three phase-ac voltage. The input voltage,  $\bar{V}$ , to the inverter circuit varied from

25 to 48 volts. Three different values of  $C_c$ , 10, 20 and 30 microfarads were used which have undamped oscillation frequencies with the 1.6 millihenry inductor  $L$  of 630, 440 and 360 respectively. The output transformer impedance tap was chosen so that the reflected transducer impedance at resonance was large enough to make the inverter circuit underdamped.

#### Transmitter Driving TR-34 Transducer

Figure 7 is an impedance plot of the TR-34 transducer with a current of 0.7 rms amperes into the transducer. The maximum resistive component of the impedance is at 425 cps which will be called the resonance of the transducer. At this frequency the transducer had an appreciable inductive component. Other minor resonances are seen at higher frequencies. The output transformer of the inverter was set at a match of 12 ohm center-tapped to 150 ohms giving a reflected impedance across the primary half winding of 10 ohms at the resonant frequency. With a value of 30 microfarads for  $C_c$ , the input voltage and current to the inverter circuit and the voltage on the 2N688 controlled rectifiers are shown in figure 8. The input voltage (a) shows a periodic variation at twice the inverter frequency. Comparing it with the input current (b), it appears that the rectifier supply has an effective inductive impedance which is causing the sawtooth waveform on the input voltage. The anode-to-cathode voltage on the silicon controlled rectifiers (c) shows clearly the two halves of the inverter period. During the first half of the period the controlled rectifier conducts current with about a one-volt drop. During the next half period the controlled rectifier blocks current and the voltage across it is the transformer primary voltage which initially is negative. The peak forward voltage is equal to the peak reverse voltage and this was found to be true as long as the transducer power factor was near unity. At lower power factors the peak reverse voltage is appreciably less than the peak forward voltage.

Figures 9, 10, 11 give plots of the performance of the inverter with values of  $C_c$  of 20 and 30 microfarads. The dotted line in the plot of  $t_c/T$  represents the minimum value of commutation ratio which will provide a commutation time of twenty microseconds. With the larger value of  $C_c$  the transmitter was operated over the range of frequencies from 370 to 600 cycles per second. With twenty microfarads of  $C_c$  due to the commutation time requirement the frequency

range is limited, to from 360 to 455 cps, but the peak voltage ratio is less allowing a greater output power capability. For operating the inverter at a constant input voltage the variation of output power with frequency can be estimated from the input resistance.

Figures 12 and 13 show the transducer voltage and current waveforms at various frequencies for two values of  $C_c$ . The switching between the two states of the inverter circuit excites a ringing in the circuit formed by the transformer leakage inductance and  $C_c$ . This ringing is visible on both the current and voltage waveforms. At some frequencies the output voltage has an appreciable amount of distortion while the current does not due to the high impedance of the transducer to the harmonics of the voltage waveform. The transducer responds to current rather than voltage and it was found that the acoustic signal radiated had even less distortion than the current.

In another test of the same transducer, an air-filled rubber pancake-like device was placed on one side of the transducer to act as a pressure release. The impedance circle taken at a current level of 0.7 amperes (figure 14) is nearly the same as for the transducer alone with the resonant frequency being increased to 440 cps. The impedance match on the output transformer was 12 ohms center-tapped to 62.5 ohms giving a reflected impedance to the inverter of 22 ohms. The commutation capacitor  $C_c$  was reduced to ten microfarads. Range of frequency of operation was possible from 441 to about 470 cps. The upper limit on the frequency is due to the fact that the commutation ratio is becoming too small to provide sufficient commutation time. The lower frequency limitation is due to the inverter input current decreasing until during part of the cycle it drops to zero which immediately allows the 2N1913 to cease to conduct. By adding a capacitor  $C_T$  in series with the transducer to balance the inductive component of the transducer, the frequency range of operation is increased. The effect of different values of  $C_T$  on the performance of the inverter unit is shown in figures 15, 16 and 17.

Figure 18 shows the transducer current and voltage waveshapes with a value of two microfarads for  $C_T$  to balance most of the inductive component of the transducer. The accelerometer voltage from an accelerometer on the transducer face is becoming distorted at resonance indicating this is near maximum drive that can be applied to the transducer. The hydrophone voltage does not yet show any distortion but slightly increasing the drive produces a severe distortion.



### Test with the R-113 Transducer

The R-113 was driven in a cylindrical baffle which had been expected to improve the water loading on the transducer. Figure 19 shows the impedance of the transducer as measured at a constant current of 1.0 rms amperes with the linear amplifier drive. The transducer resonance is at 414 cps and the baffle produces another resonance at 258 cps. It was not noticed at the time this data was taken but the more complete data taken with the inverter drive indicated that at resonance the transducer current was strongly distorted even though the voltage was not. The accelerometer voltage and hydrophone voltage were monitored to observe any indication of the closing of the air gaps and these waveforms were sinusoidal. Closing of the air gaps was evident by high frequency ringing appearing on the accelerometer waveform which occurred at a current level of 1.2 amperes.

The output transformer for the inverter circuit was again set to match 12 ohms center-tapped to 62.5 ohms giving a reflected impedance of 12 ohms at resonance. The value of  $C_c$  was 20 microfarads. No series tuning was used with the transducer. The plots of the input resistance, peak voltage ratio and commutation time shown in figures 20, 21 and 22 have a similar form to those obtained with the TR-34 transducer.

In this test a more complete set of waveforms for experimental transmitter and transducer was obtained. The top row of pictures in figure 23 shows the transducer voltage and current. The current becomes strongly distorted at the resonant frequency and the waveform is not symmetric with respect to the positive and negative portion of the waveform. This distortion does not appear on the transducer accelerometer voltage or hydrophone voltage (middle row of pictures, figure 23) so the mechanical motion of the transducer remains sinusoidal. The inverter circuit has two symmetric states so it should not produce the type of distortion appearing in the transducer current waveform. This leaves as the most likely cause of the distortion the magnetic circuit of the transducer and particularly the permanent magnetic bias. The bottom row of pictures in figure 23 shows the input voltage and current waveforms to the inverter circuit. The small discontinuity appearing in the voltage waveform is due to the commutation of current between rectifiers in the rectifier bridges occurring 720 times per second. The inverter input current waveform at 400 cps drops to nearly zero at the end of the half period. When the

operating frequency was lowered below 400 cps the current does drop to zero which allows the 2N1913 controlled rectifier to turn off and the inversion process is stopped. As the frequency is increased above 400 cps, the input current no longer approaches zero. The upper limit on the operating frequency is due to the decreasing commutation ratio resulting chiefly from the decreasing transducer impedance.

## SUMMARY OF RESULTS

The performance of the transmitter reported in the preceding section demonstrated that it could efficiently supply a nearly sinusoidal voltage to a medium  $Q$  transducer. The small amount of harmonic voltage, principally third, in the output voltage from the transmitter did not appear in the acoustic output from the transducer. The transducer efficiency and radiated beam pattern were found to be the same for equal drive currents with both the experimental transmitter and a sinusoidal drive from a linear amplifier. Values of transmitter efficiency ranged from 60 to 75 percent with the efficiency increasing as the output power was increased. At full power the transmitter efficiency is expected to be 80 percent. Because the transducers became non-linear at input power levels greater than 300 watts, the transmitter output power was limited to this level. No difficulty is expected from increasing the transmitter output power to its full capacity of 2000 watts if transducer loads are available.

The value of  $L$  and  $C_c$  used in the inverter circuit were chosen such that the circuit was underdamped and the period of oscillation between  $L$  and  $C_c$  was approximately equal to the resonant frequency of the transducer (see equations 1 and 2). The output voltage from the transmitter operating at the resonant frequency was then nearly sinusoidal. At frequencies greater than the resonant frequency of the transducer the waveform became strongly distorted due probably to the decrease in the transducer impedance. The value of  $C_c$  used in most of the tests was such that its impedance,  $1/4\omega C_c$ , across one of the primary half windings was half the reflected transducer impedance at resonance. With this value of  $C_c$ , it was possible to operate the transmitter over the range of frequencies between the quadrature points of the transducer.

The plots of  $k$  and  $R_{in}$  indicate how the output voltage and power are changing with frequency. At resonance, with the transducer power factor corrected to near unity if necessary, the inverter input resistance  $R_{in}$  was about one-third the reflected transducer impedance, and peak voltage ratio was five to six. Using a value of transmitter



efficiency of 75 percent and substituting equations (5) and (6) into equation (3) gives the maximum output power of the transmitter as

$$0.75 \left( \frac{V_p}{k} \right) \left( \frac{I_{rms}}{\frac{\pi}{4}} \right).$$

In terms of the voltage and current ratings of one of the controlled rectifiers in the inverter circuit the maximum output power is approximately

$$\frac{(V_{bo})(I_{rms})}{5}.$$

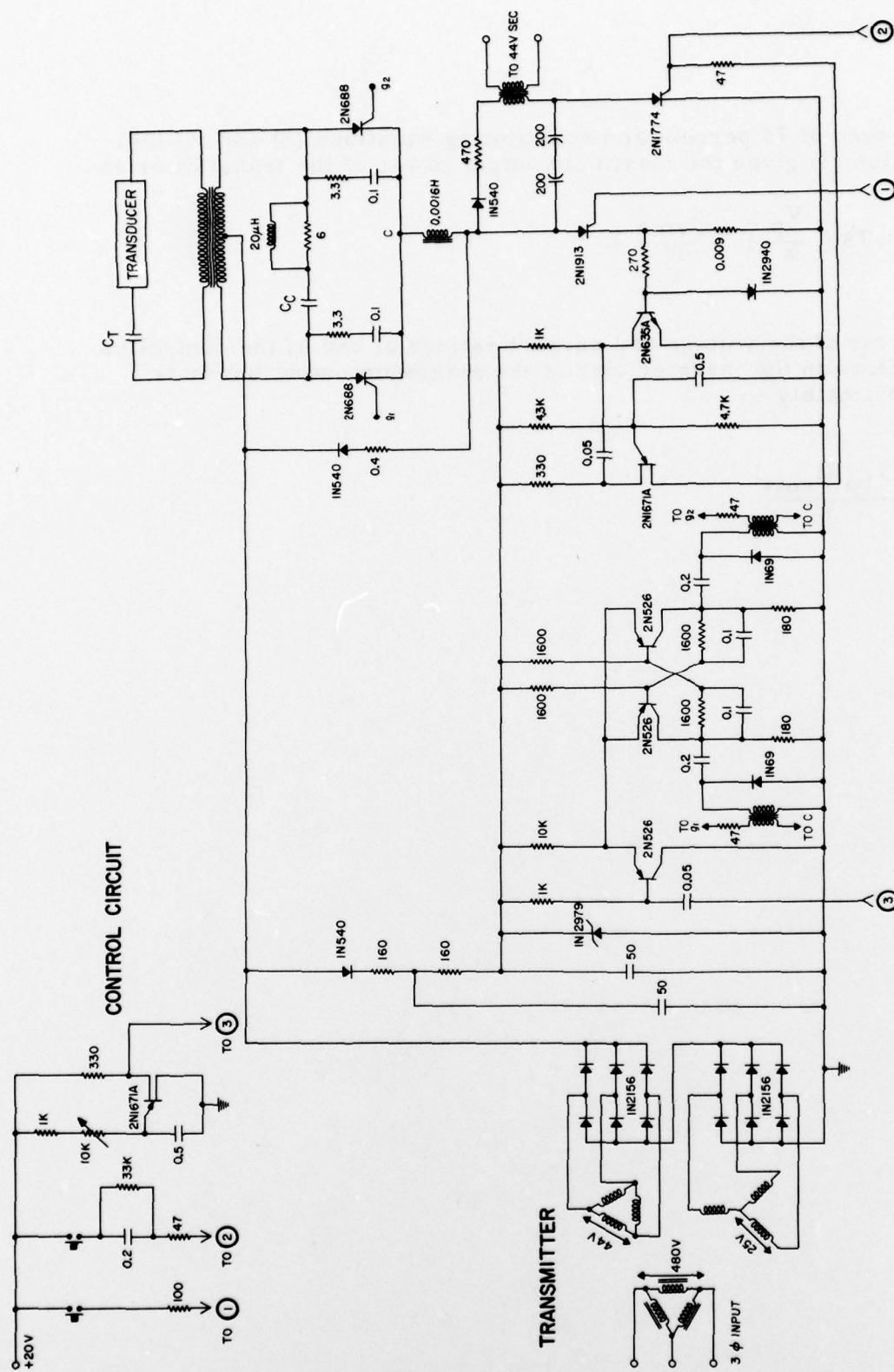


Figure 1 - Circuit for experimental sonar transmitter

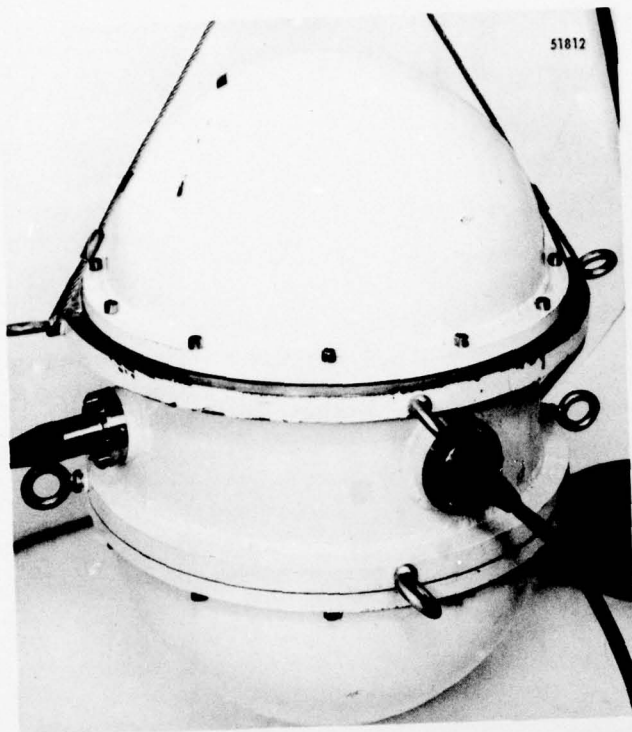


Figure 2 - Exterior view  
of submersible vessel  
containing transmitter

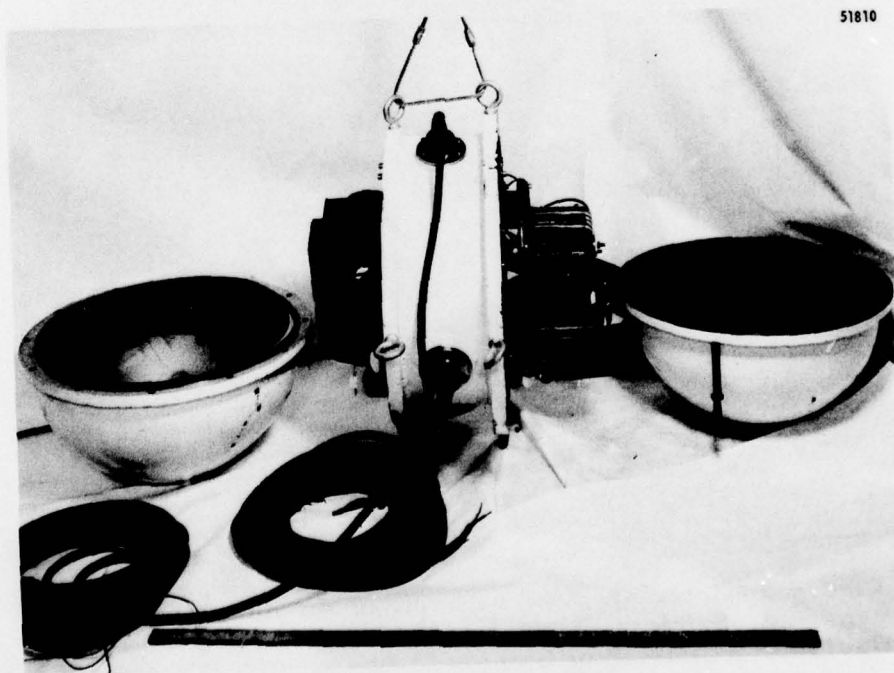


Figure 3 - Center section of vessel with two end domes removed

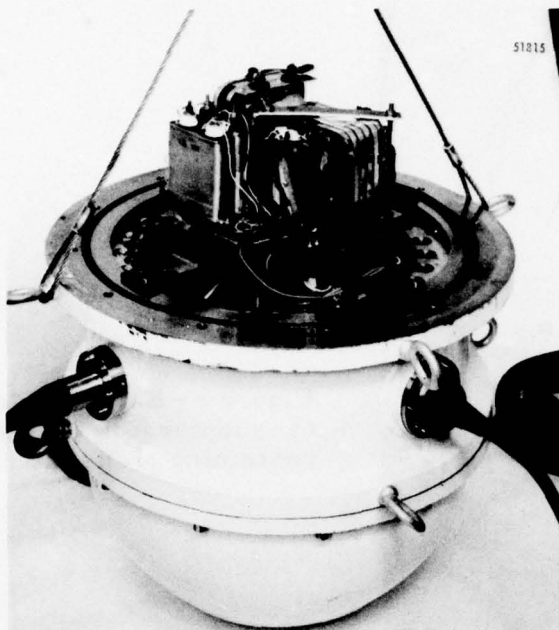


Figure 4 - View showing one of the mounting plates for large components

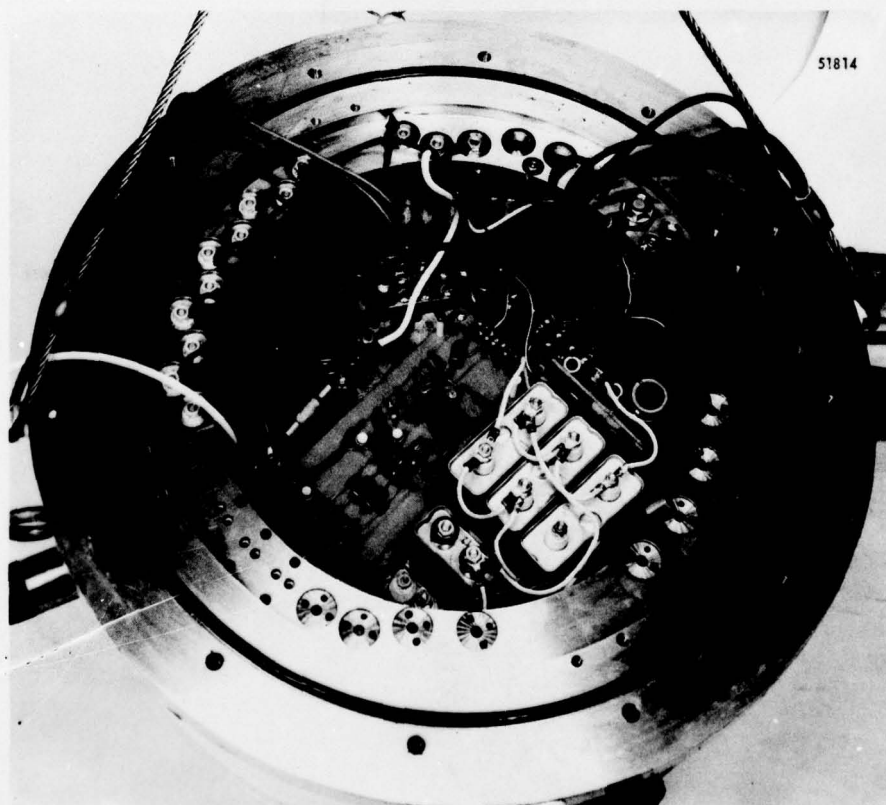
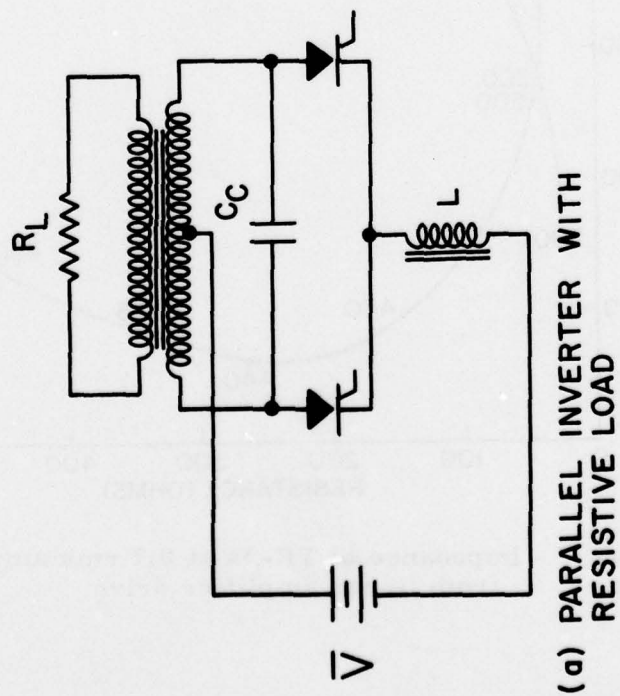
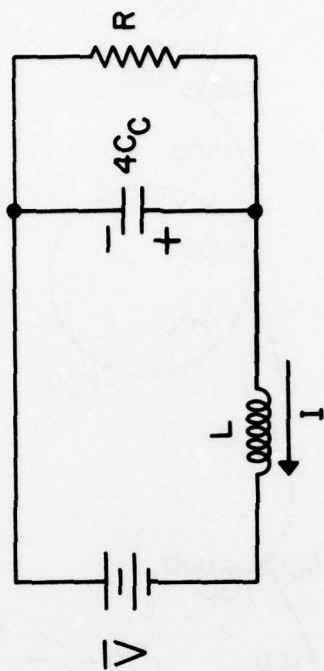


Figure 5 - Interior view with one of the mounting plates removed. Semiconductor components are mounted along the inner extension of flange.





(a) PARALLEL INVERTER WITH RESISTIVE LOAD



(b) HALF PERIOD EQUIVALENT CIRCUIT

Figure 6 - Parallel inverter circuit



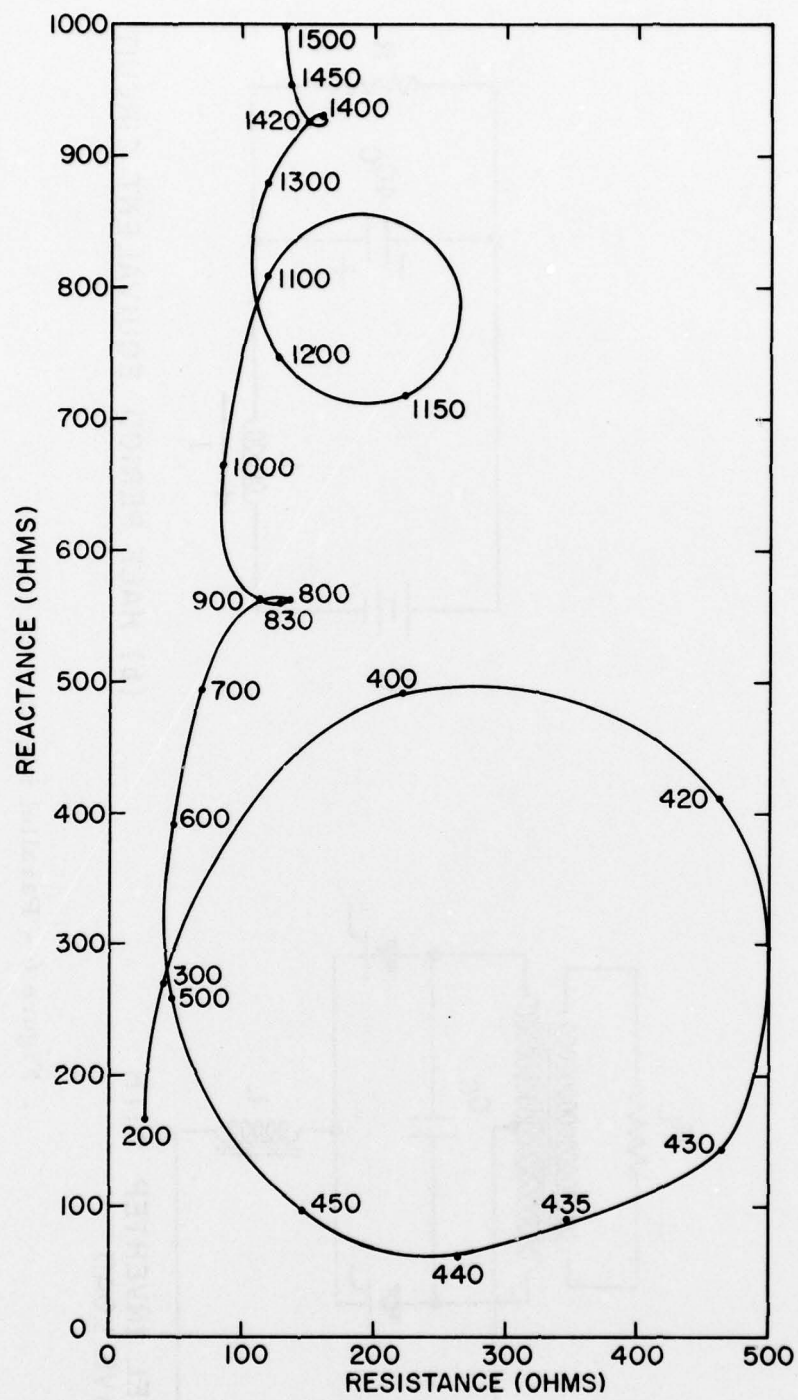
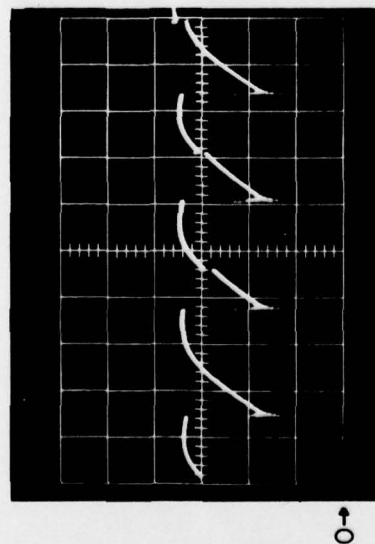
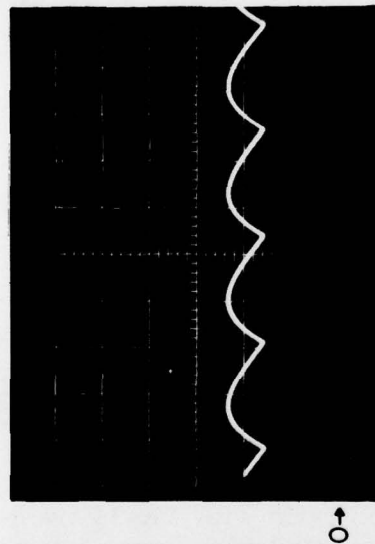


Figure 7 - Impedance of TR-34 at 0.7 rms amperes from linear amplifier drive



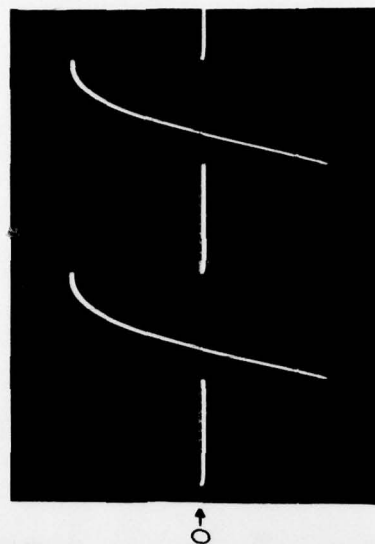
VERTICAL SCALE 8 VOLTS/DIV  
HORIZONTAL SCALE 0.5 MILLI SEC/DIV

Figure 8a - DC input voltage  
to inverter circuit



VERTICAL SCALE 5 AMP/DIV  
HORIZONTAL SCALE 0.5 MILLI SEC/DIV

Figure 8b - DC input current  
to inverter circuit



VERTICAL SCALE 40 VOLTS/DIV  
HORIZONTAL SCALE 0.5 MILLI SEC/DIV

Figure 8c - Controlled rectifier voltage  
anode to cathode

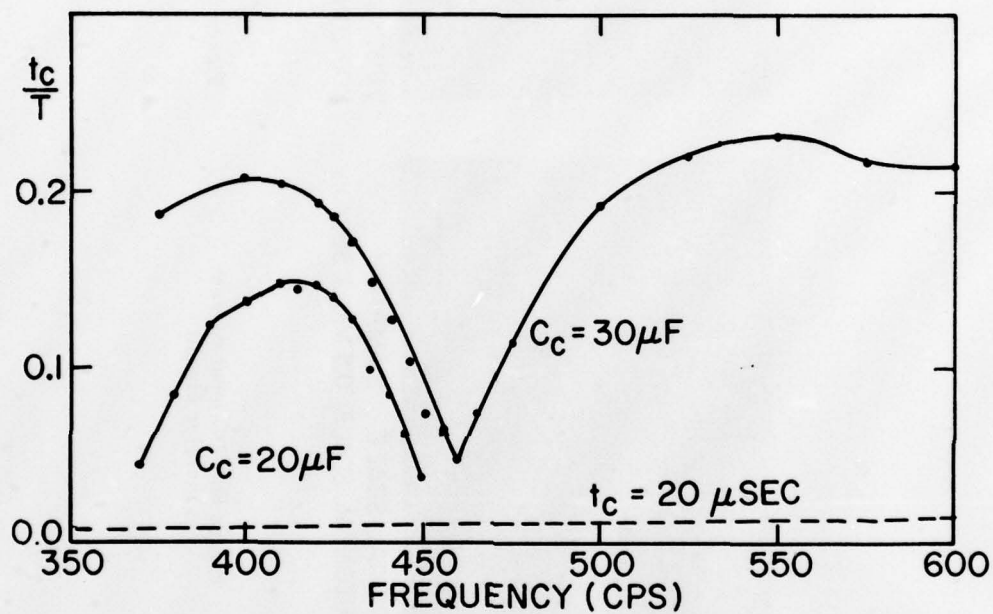


Figure 9 - Commutation ratio with TR-34 transducer as a load at a current level of 0.7 rms amperes



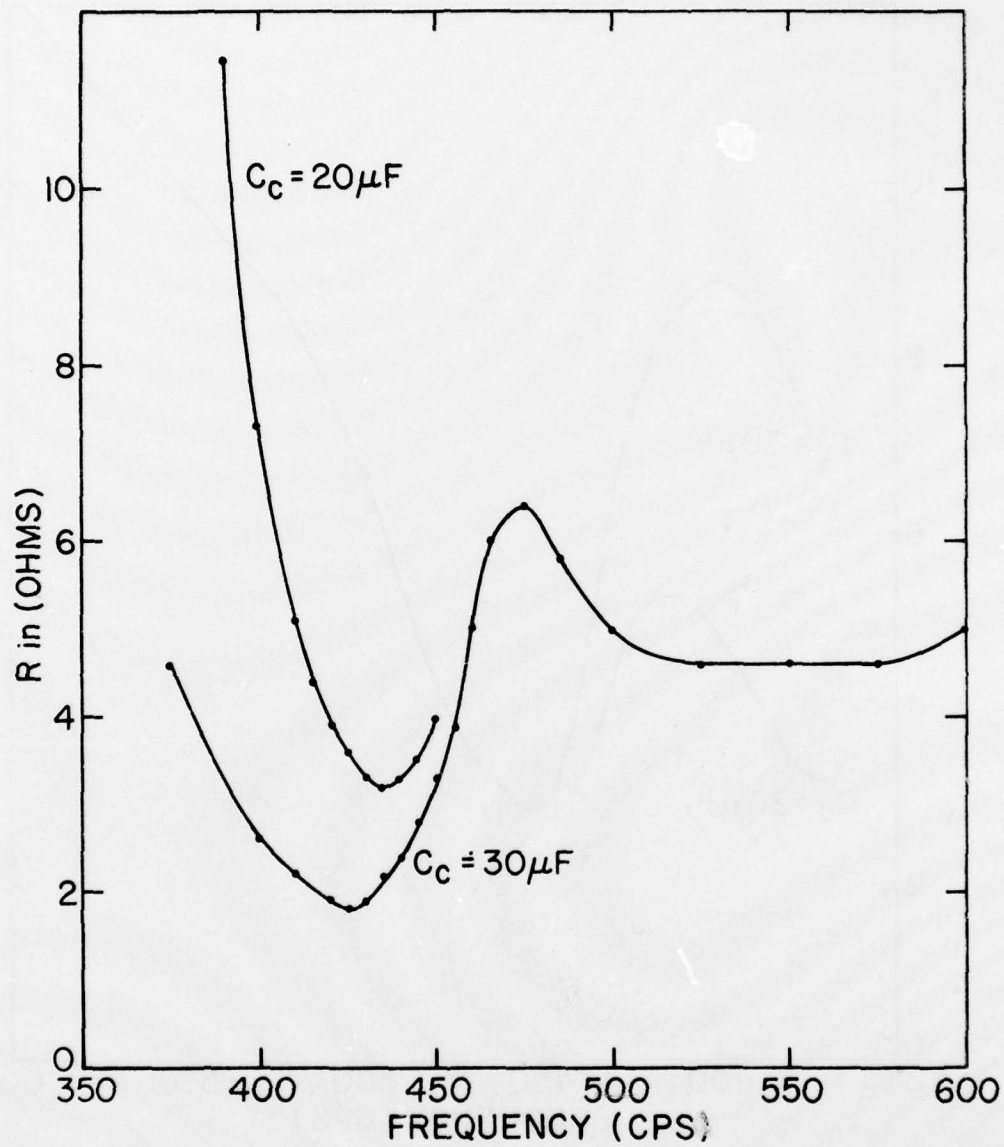


Figure 10 - Input resistance

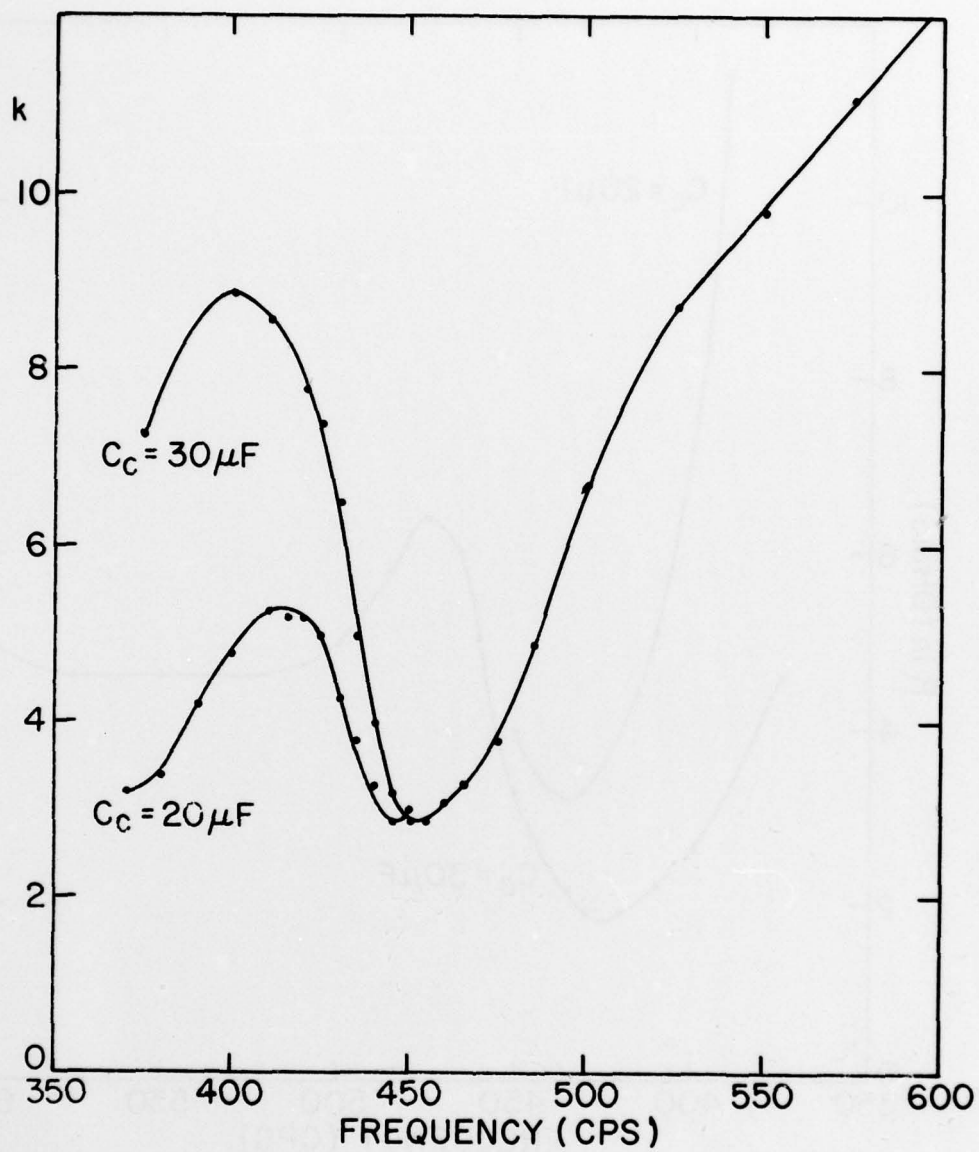


Figure 11 - Peak voltage ratio

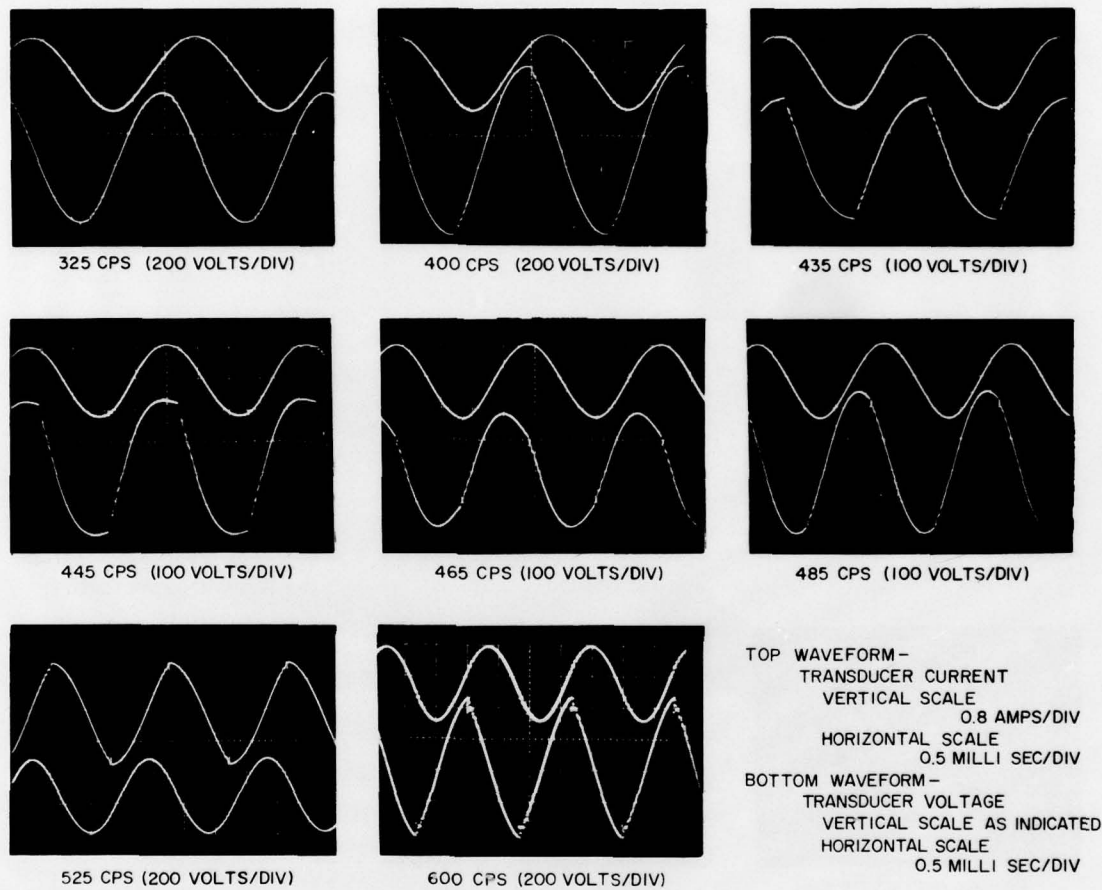


Figure 12 - Transducer voltage and current waveforms with experimental transmitter drive and  $C_c = 30$  microfarads



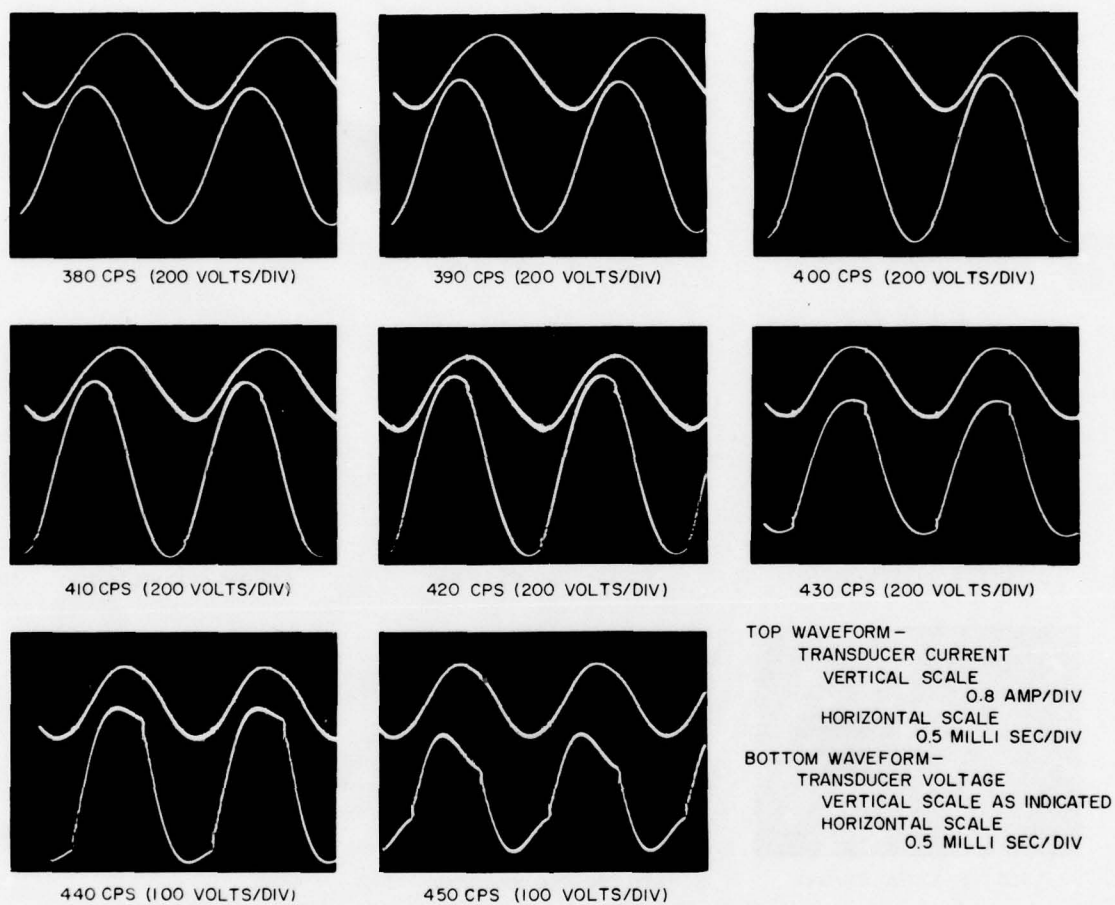


Figure 13 - TR-34 transducer voltage and current waveforms with experimental transmitter drive and  $C_c = 20$  microfarads

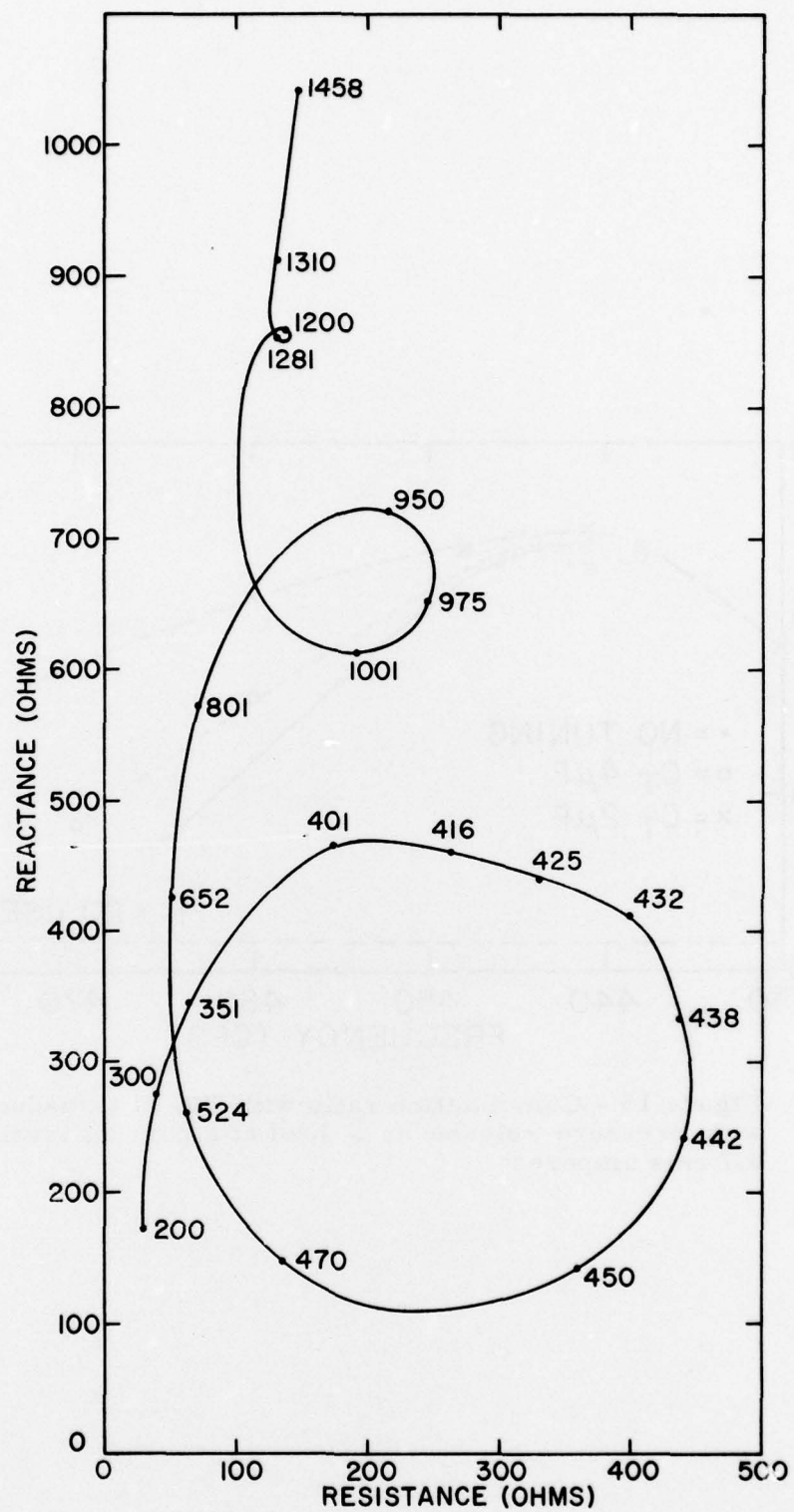


Figure 14 - Impedance of TR-34 with pressure release at 0.7 rms amperes from linear amplifier drive

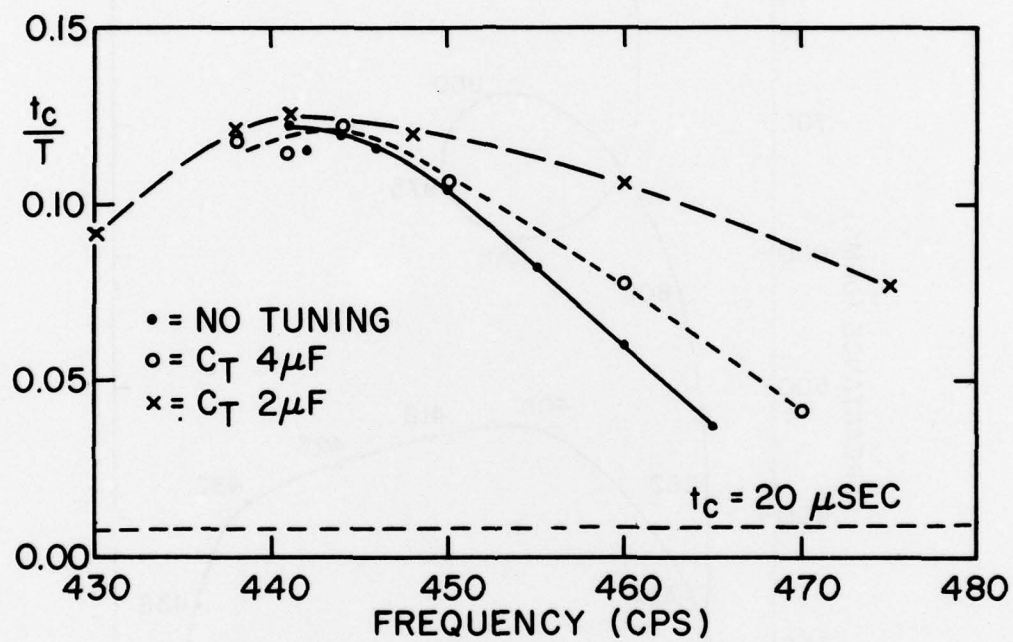


Figure 15 - Commutation ratio with TR-34 transducer with pressure release as a load at a current level of 0.7 rms amperes



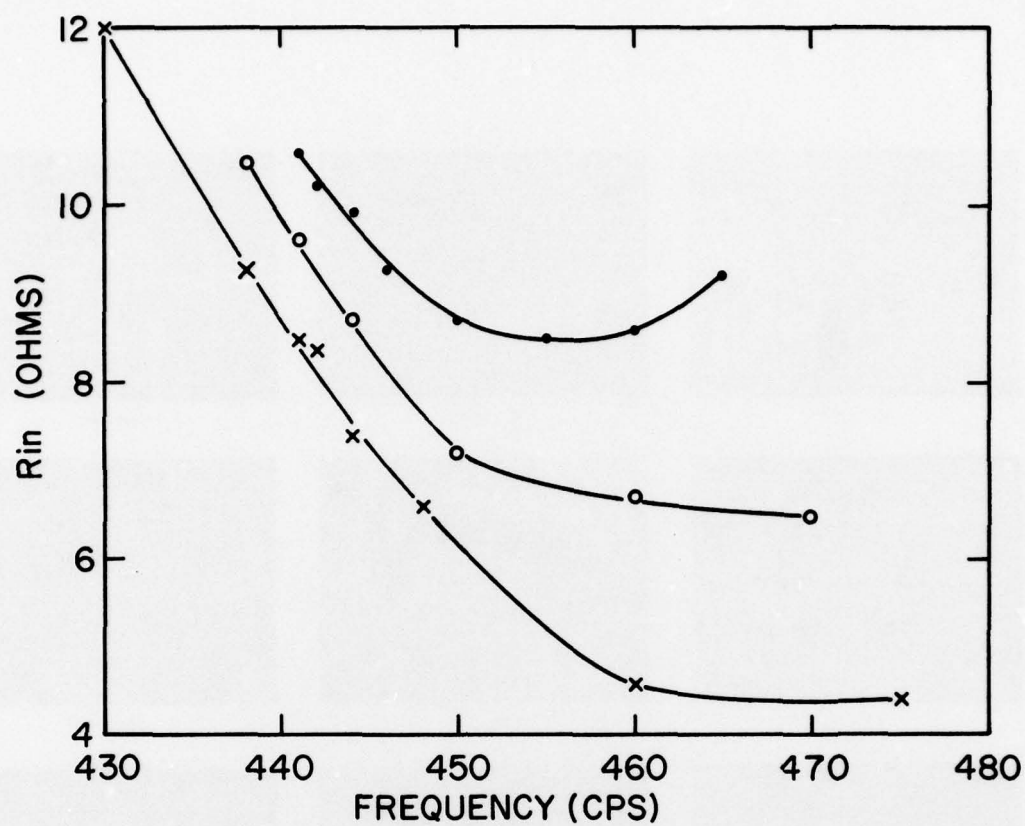


Figure 16 - Input resistance

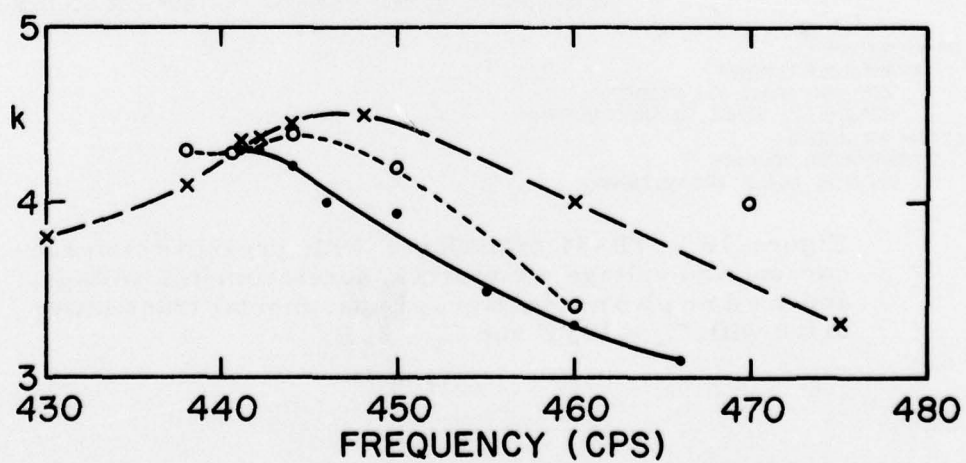
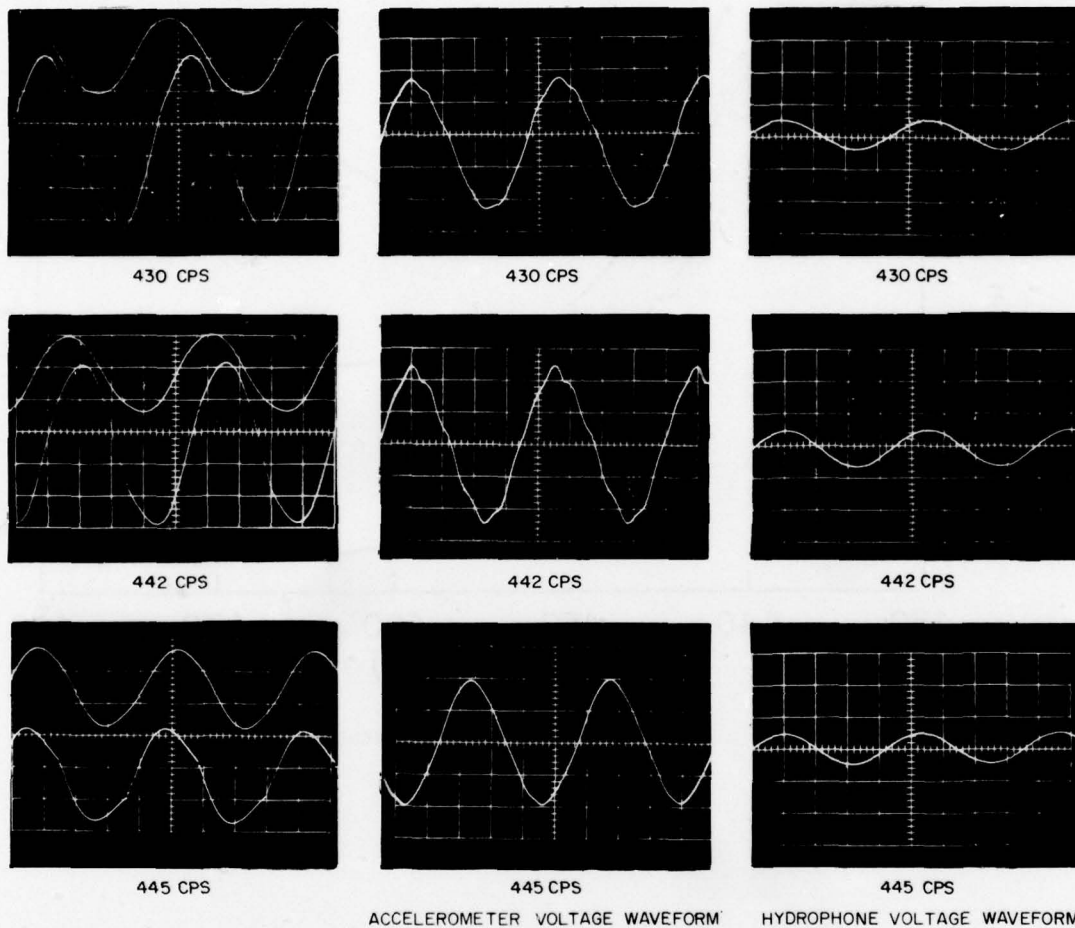


Figure 17 - Peak voltage ratio



TOP WAVEFORM -  
 TRANSDUCER CURRENT  
 VERTICAL SCALE 0.8 AMPS/DIV  
 HORIZONTAL SCALE 0.5 MILLI SEC/DIV

BOTTOM WAVEFORM -  
 TRANSDUCER VOLTAGE  
 VERTICAL SCALE 200 VOLTS/DIV

Figure 18 - TR-34 transducer with pressure release current and voltage waveforms, accelerometer voltage, and hydrophone voltage. Experimental transmitter drive with  $C_c = 10 \mu F$  and  $C_t = 2 \mu F$ .

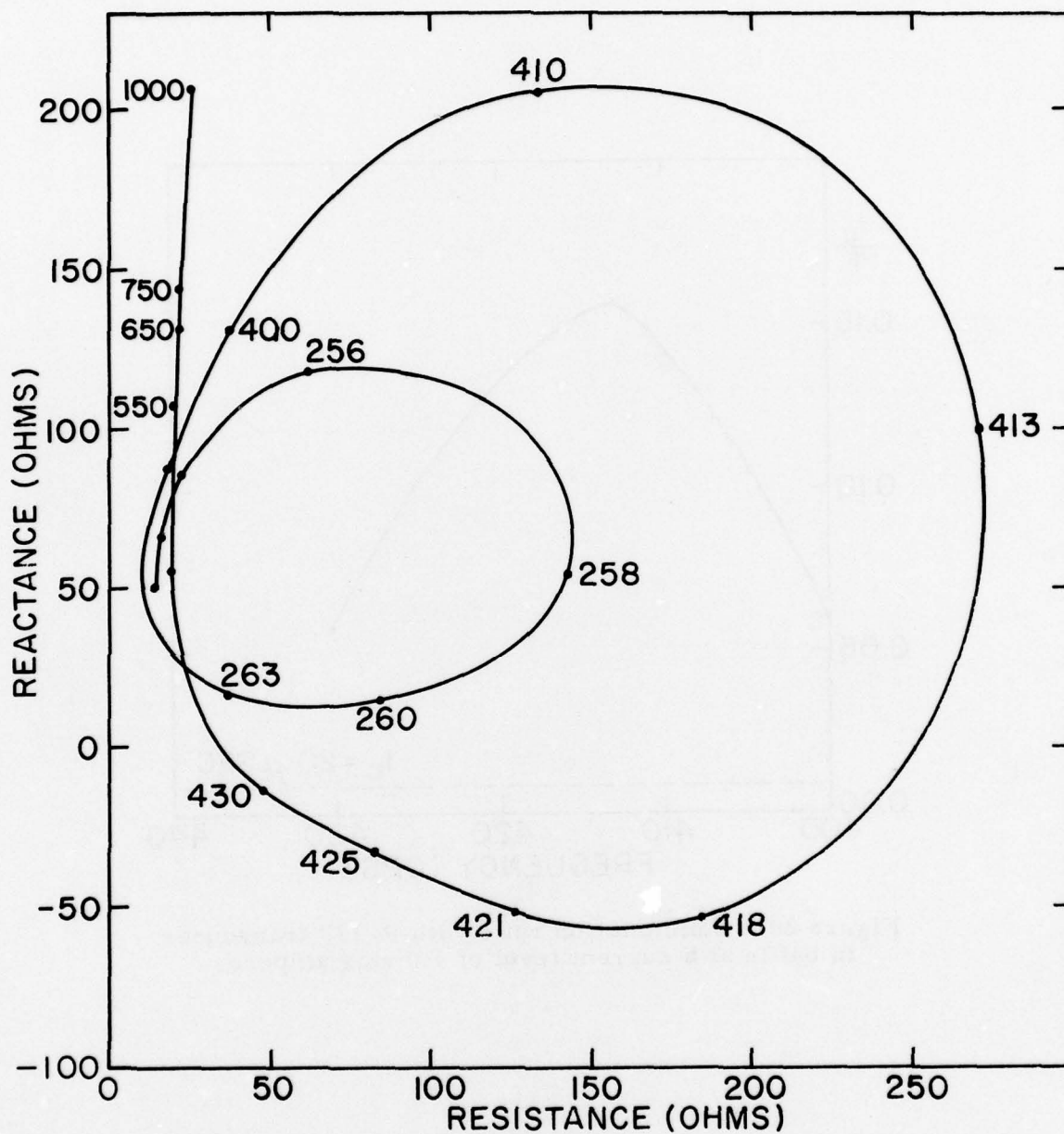


Figure 19 - Impedance of R-113 in baffle at 1.0 rms amperes from linear amplifier drive



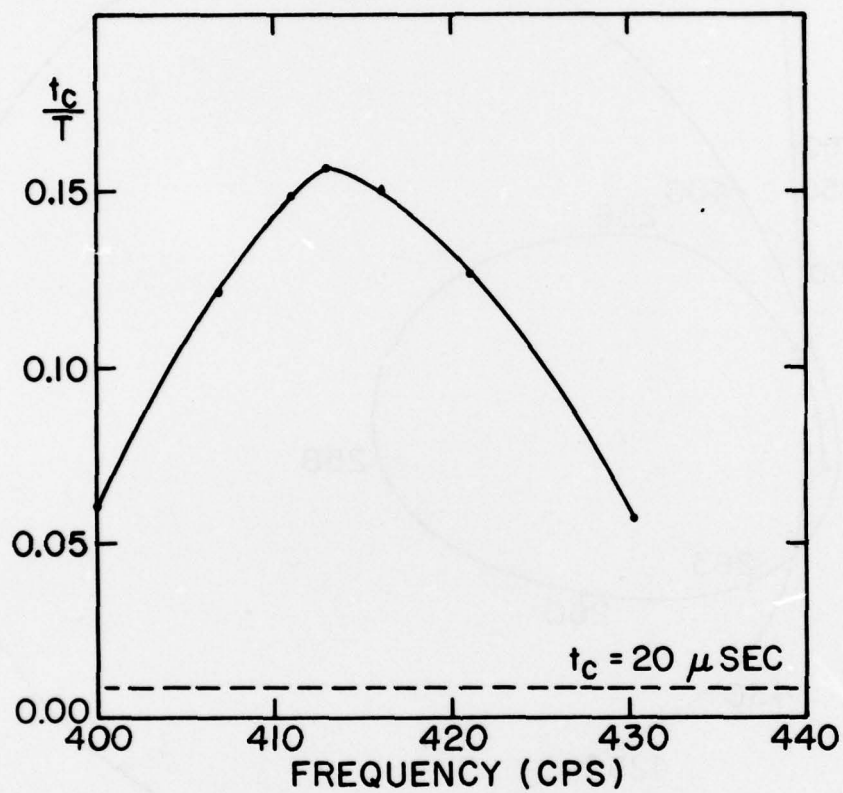


Figure 20 - Commutation ratio with R-113 transducer  
in baffle at a current level of 1.0 rms amperes

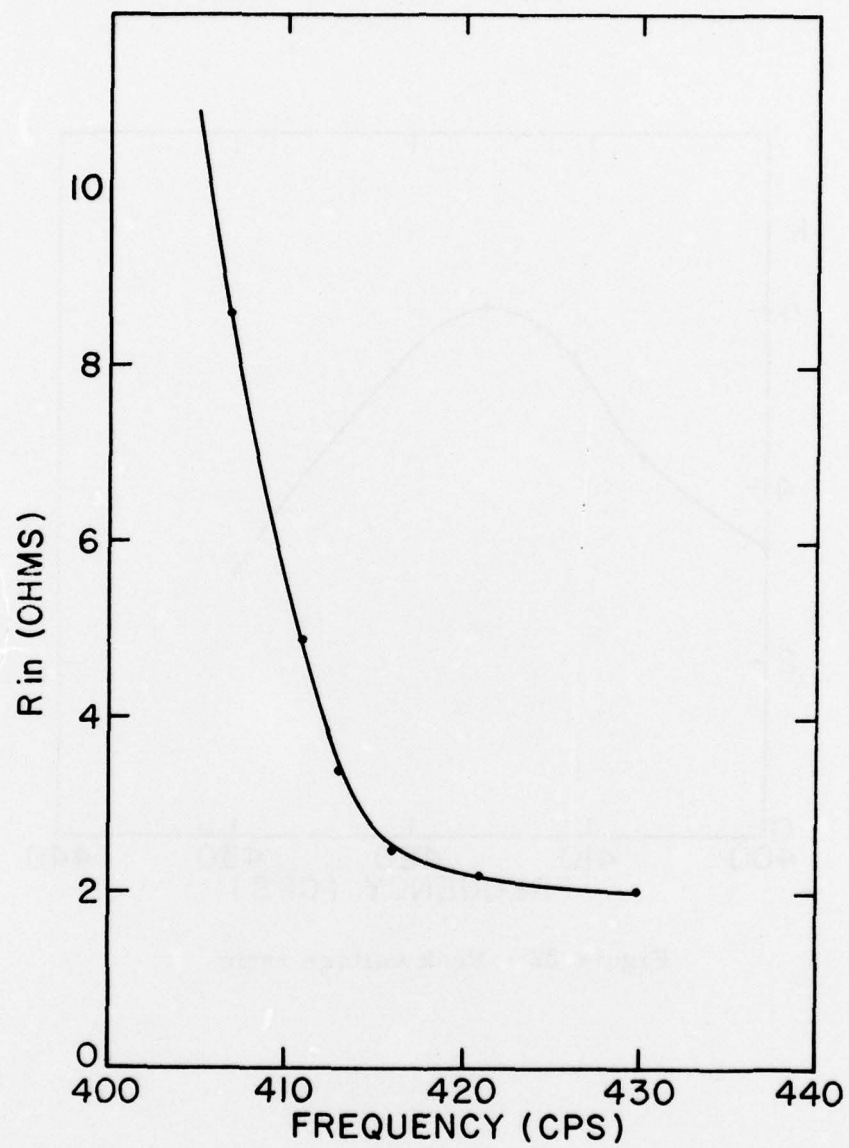


Figure 21 - Input resistance

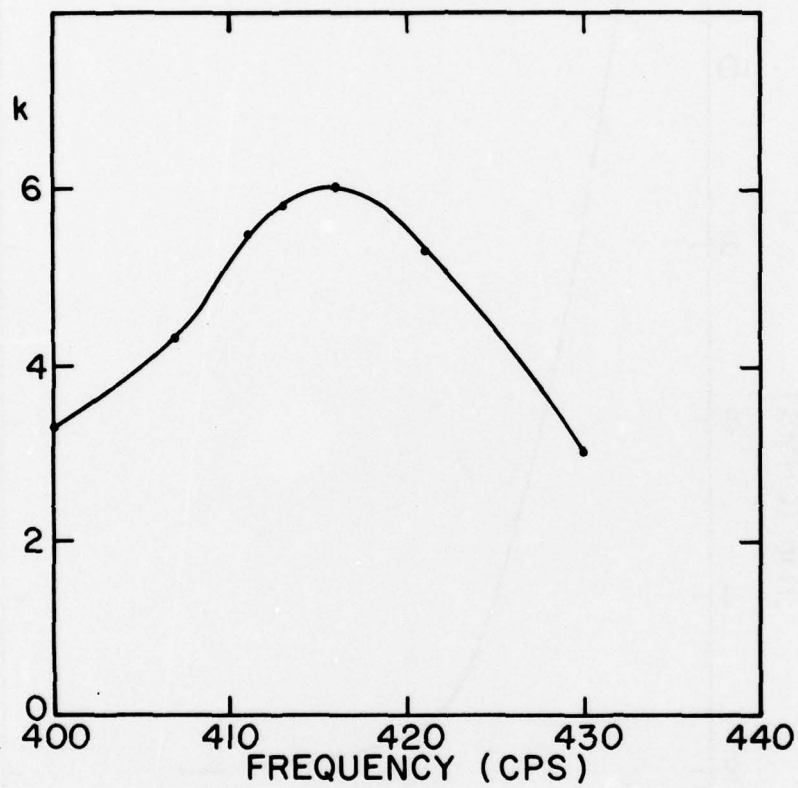
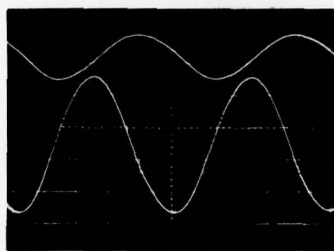
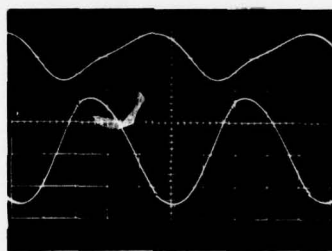


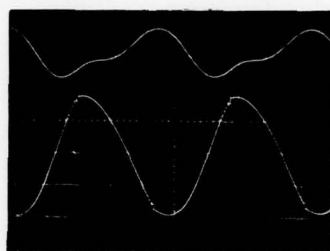
Figure 22 - Peak voltage ratio



400 CPS (100 VOLTS/DIV)

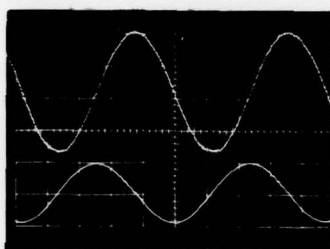
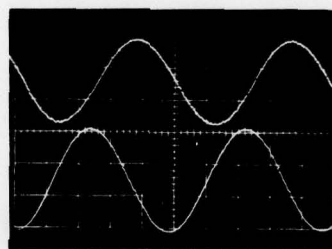
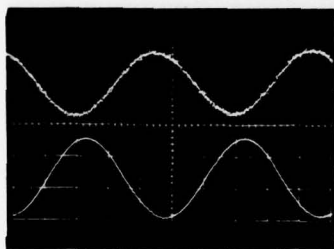


411 CPS (200 VOLTS/DIV)

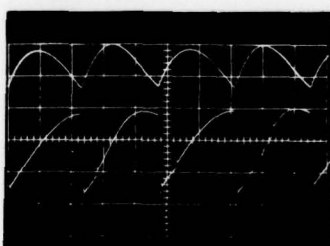
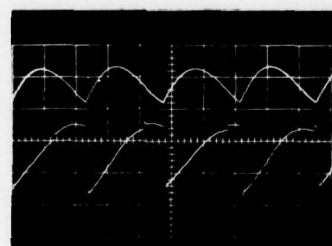
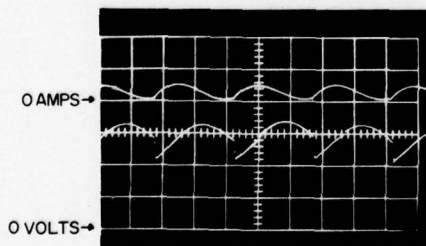


413 CPS (200 VOLTS/DIV)

TOP WAVEFORM—  
 TRANSDUCER CURRENT  
 VERTICAL SCALE 2 AMP/DIV  
 HORIZONTAL SCALE 0.5 MILLI SEC/DIV  
 BOTTOM WAVEFORM—  
 TRANSDUCER VOLTAGE  
 VERTICAL SCALE AS INDICATED



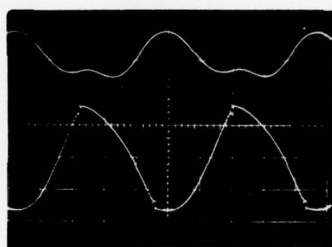
TOP WAVEFORM—  
 HYDROPHONE VOLTAGE WAVEFORM  
 BOTTOM WAVEFORM—  
 ACCELEROMETER VOLTAGE WAVEFORM



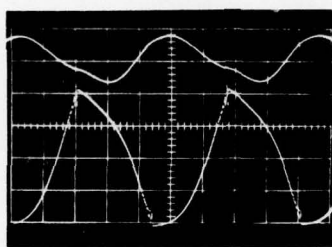
TOP WAVEFORM—  
 INPUT CURRENT TO INVERTER  
 VERTICAL SCALE 6 AMP/DIV  
 HORIZONTAL SCALE 0.5 MILLI SEC/DIV  
 BOTTOM WAVEFORM—  
 INPUT VOLTAGE TO INVERTER  
 VERTICAL SCALE 10 VOLTS/DIV

Figure 23 - Waveforms for experimental transmitter with  $C_c = 20$  microfarads driving R-113 transducer in baffle

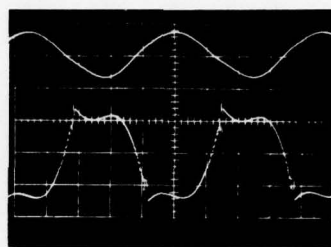




416 CPS (200 VOLTS)



421 CPS (100 VOLTS)



430 CPS (50 VOLTS)

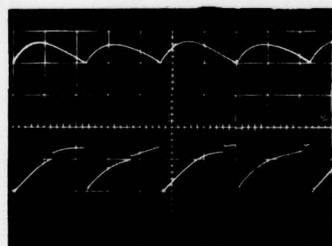
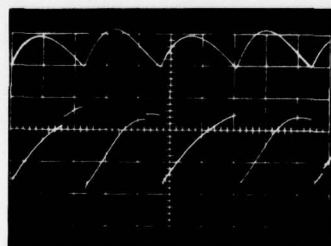
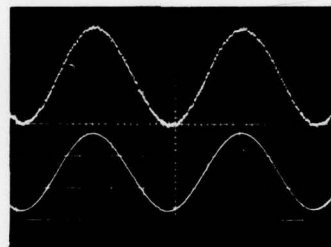
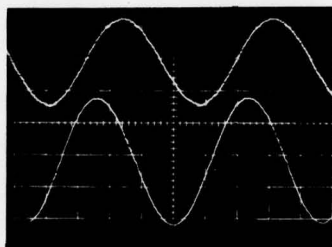
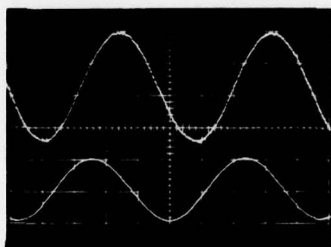


Figure 23 (continued) - Waveforms for experimental transmitter with  $C_C = 20$  microfarads driving R-113 transducer in baffle

## APPENDIX

This appendix contains data taken on the transducer loads driven with a sine wave of voltage from a vacuum tube linear amplifier. Section A is data on the TR-34 transducer; section B, the TR-34 with pressure release assembly; and section C, the R-113 in cylindrical baffle. Each section contains the following parts.

1. Drawing or photograph showing orientation of transducer.
2. Transducer impedance versus frequency at 0.1 rms ampere current level.
3. Hydrophone voltage converted to acoustic pressure in microbars at one meter versus frequency at 0.1 rms ampere current level.
4. Beam patterns with acoustic pressure in microbars at one meter and the calculated value of transducer efficiency at resonance.

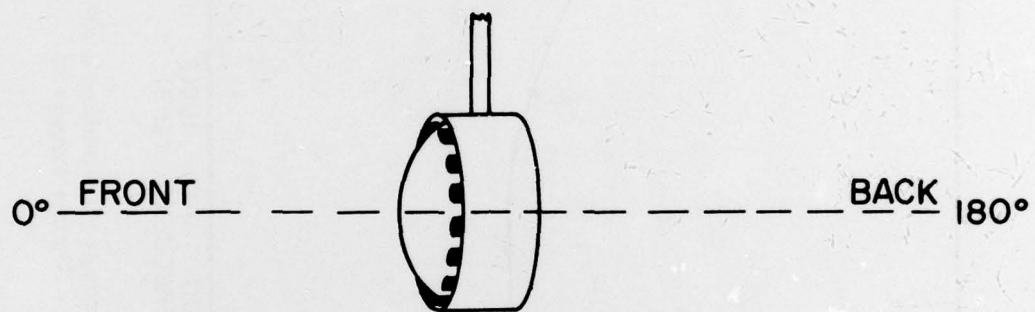


Figure A1 - Orientation of TR-34

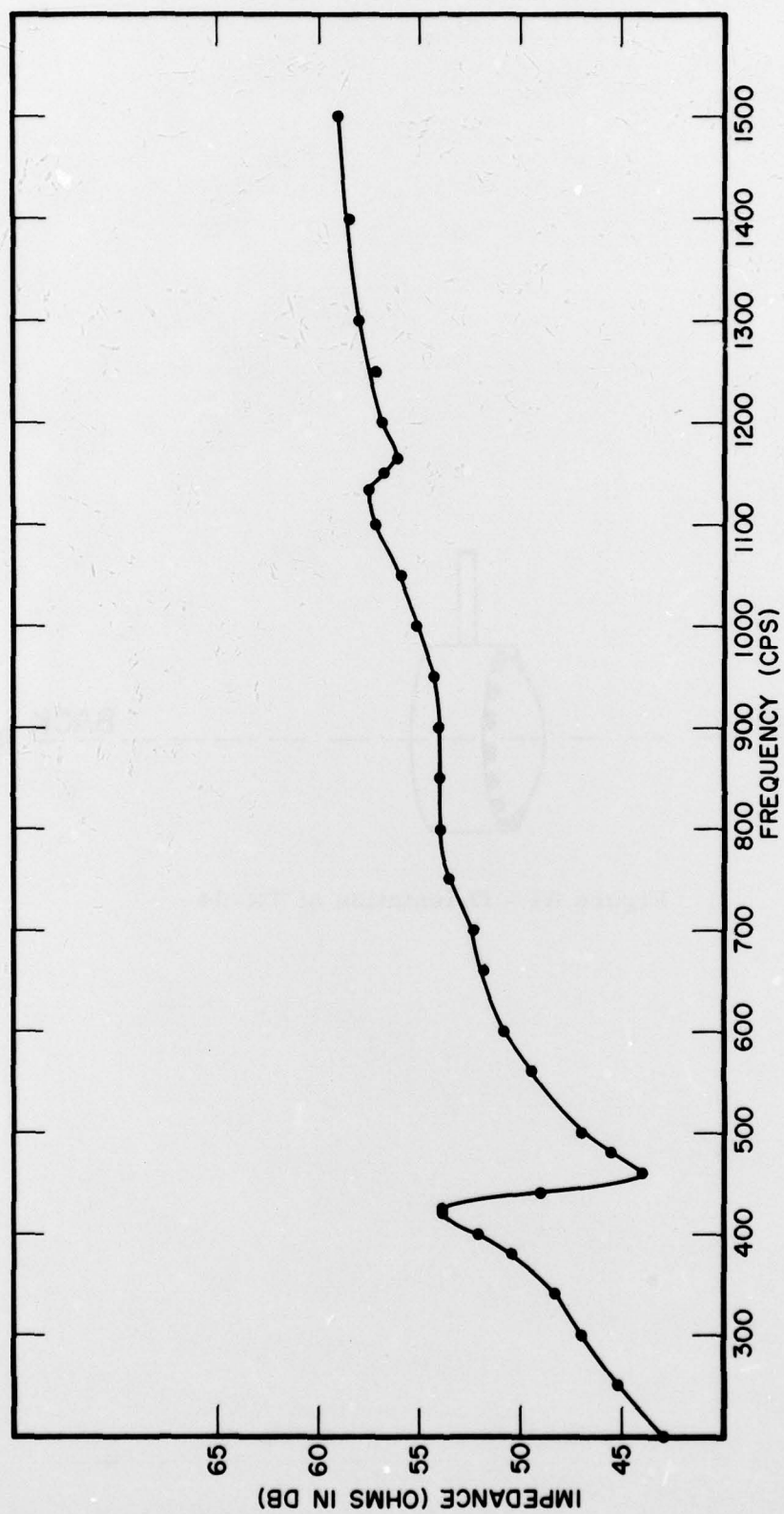


Figure A2 - Transducer impedance at current level of 0.1 rms amperes



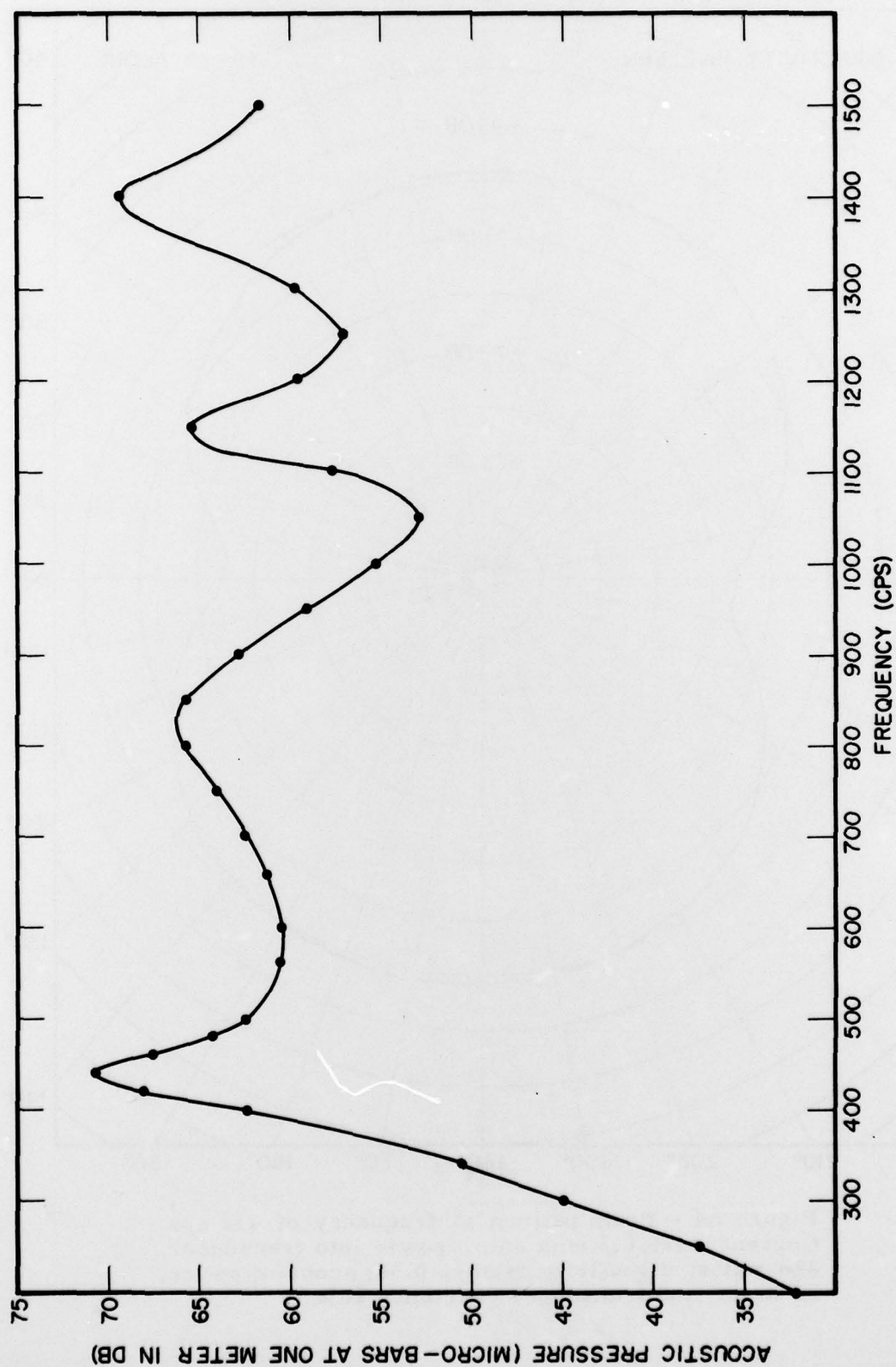


Figure A3 - Acoustic pressure in front direction at current level of 0.1 rms amperes, transducer depth 41.7 meters, hydrophone separation 8 meters

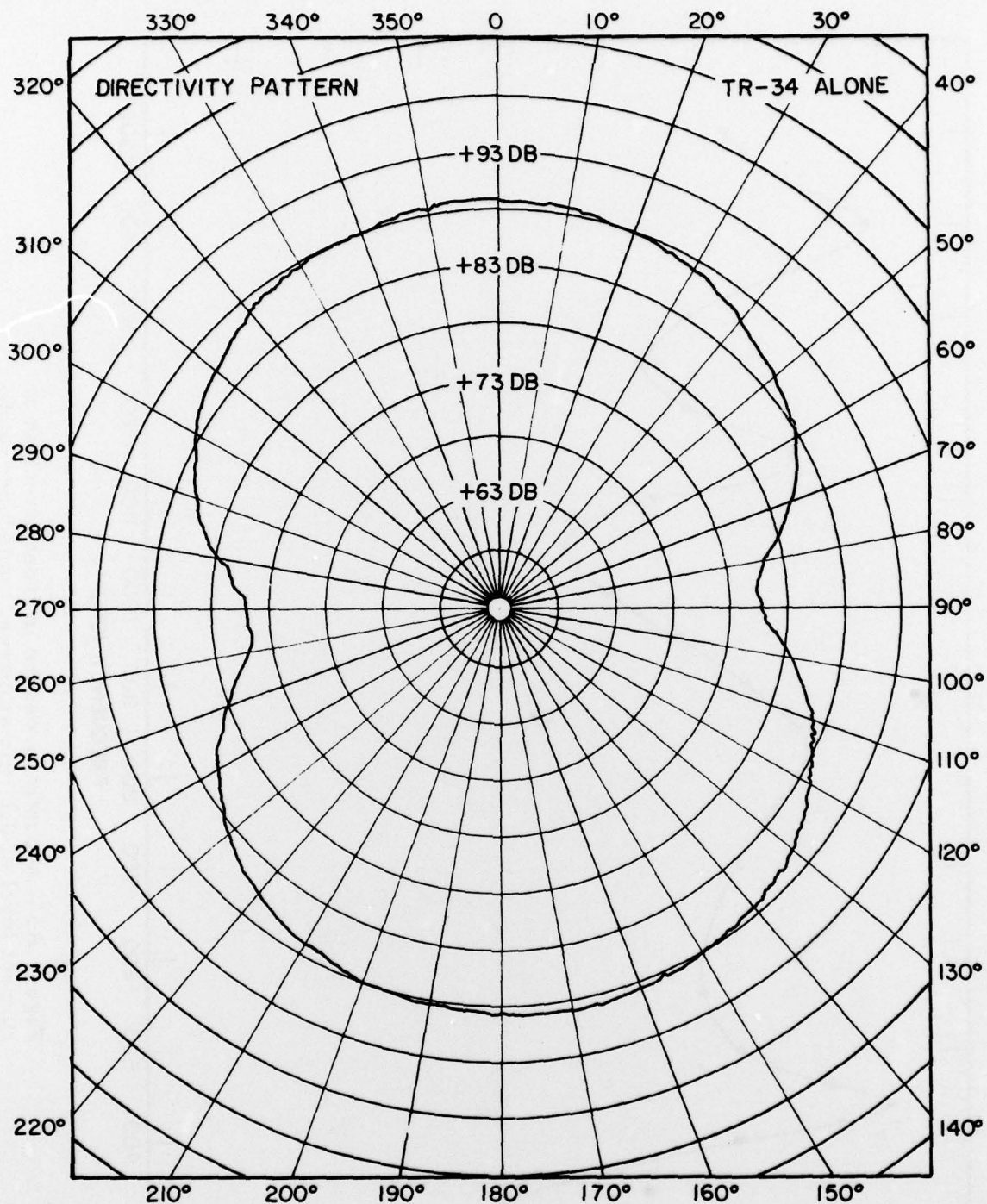


Figure A4 - Beam pattern at frequency of 432 cps.  
Current level, 0.7 rms amp.; power into transducer,  
228 watts; directivity factor, 0.36; acoustic power,  
24 watts; and transducer efficiency 10%.

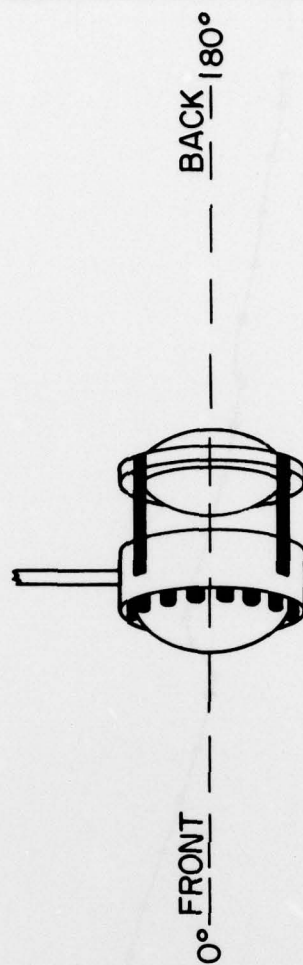
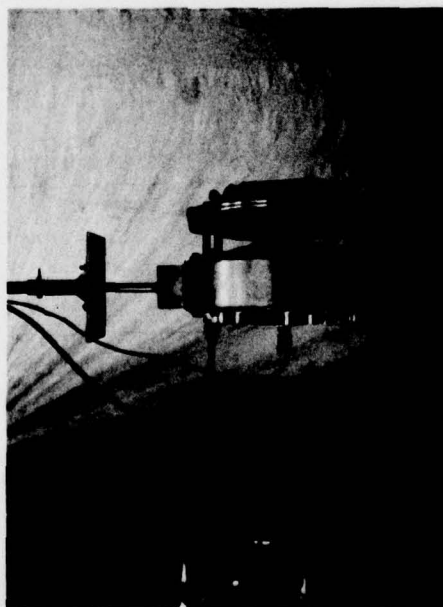


Figure B1 - Orientation of TR-34 with  
pressure release assembly



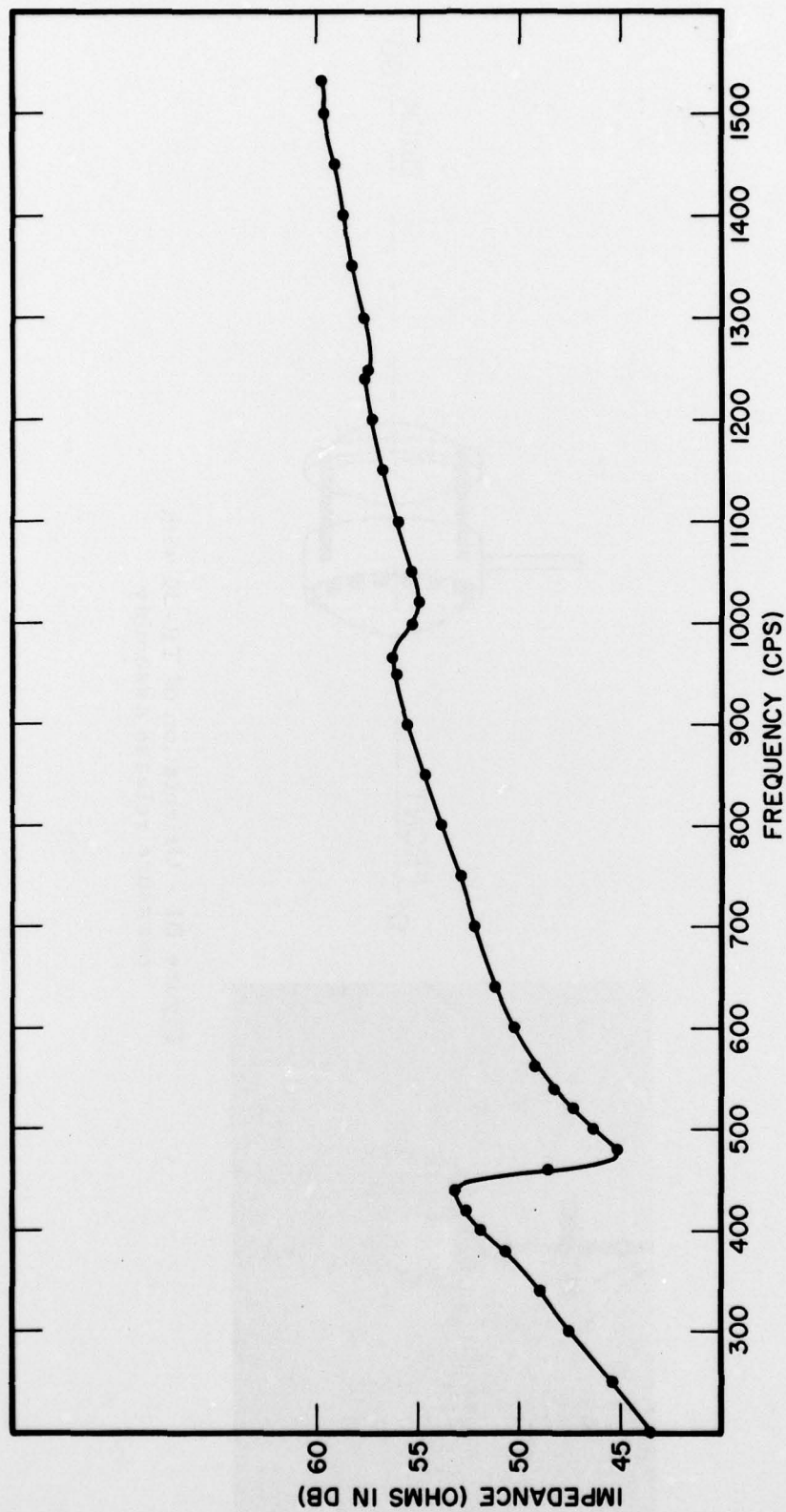


Figure B2 - Transducer impedance at current level of 0.1 rms amperes



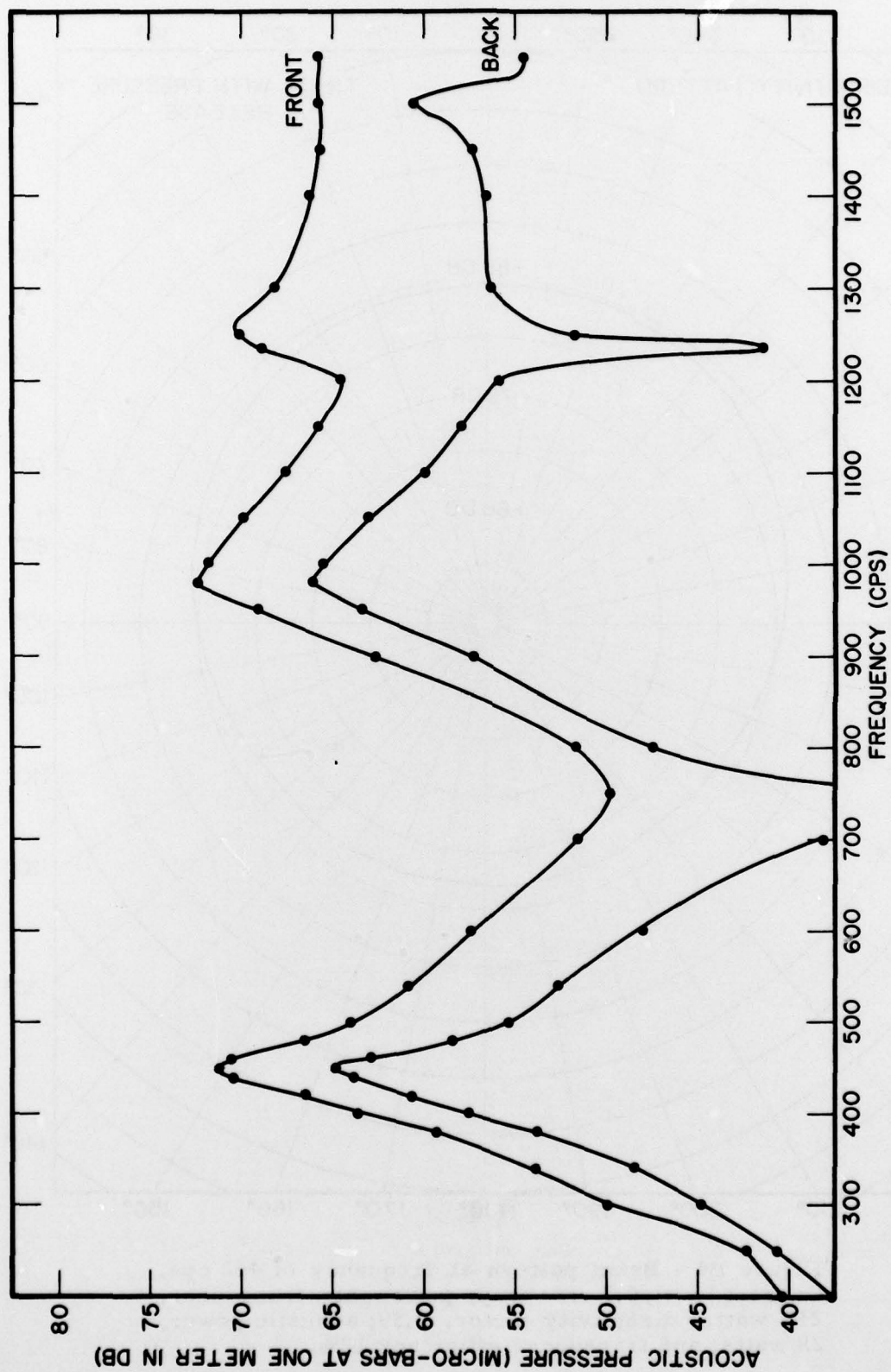


Figure B3 - Acoustic pressure in front and back direction of 0.1 rms amperes current level, transducer depth 41.7 meters, hydrophone separation 8 meters

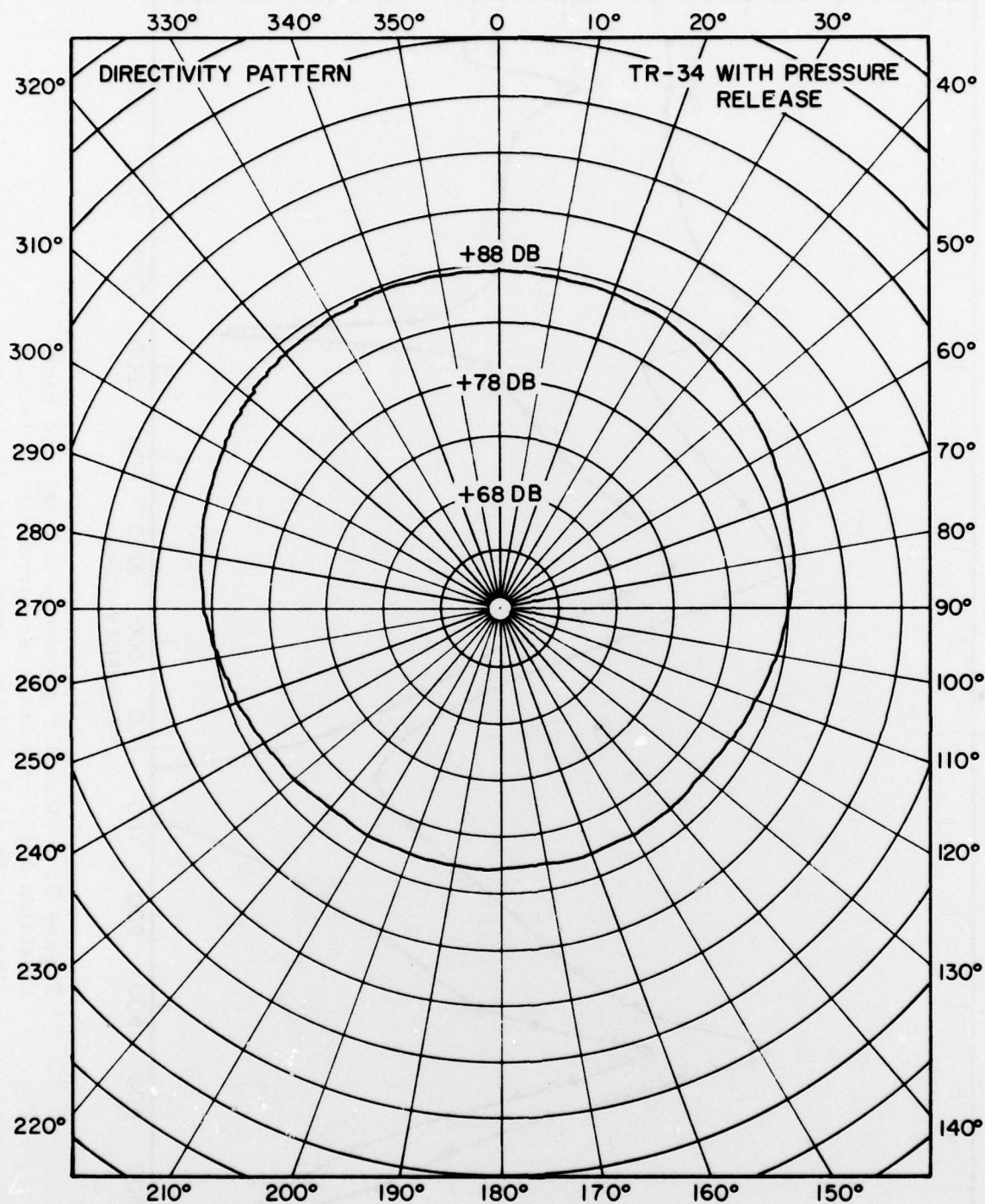


Figure B4 - Beam pattern at frequency of 442 cps. Current level, 0.7 rms amp; power into transducer, 219 watts; directivity factor, 0.39; acoustic power, 28 watts; and transducer efficiency 12%.

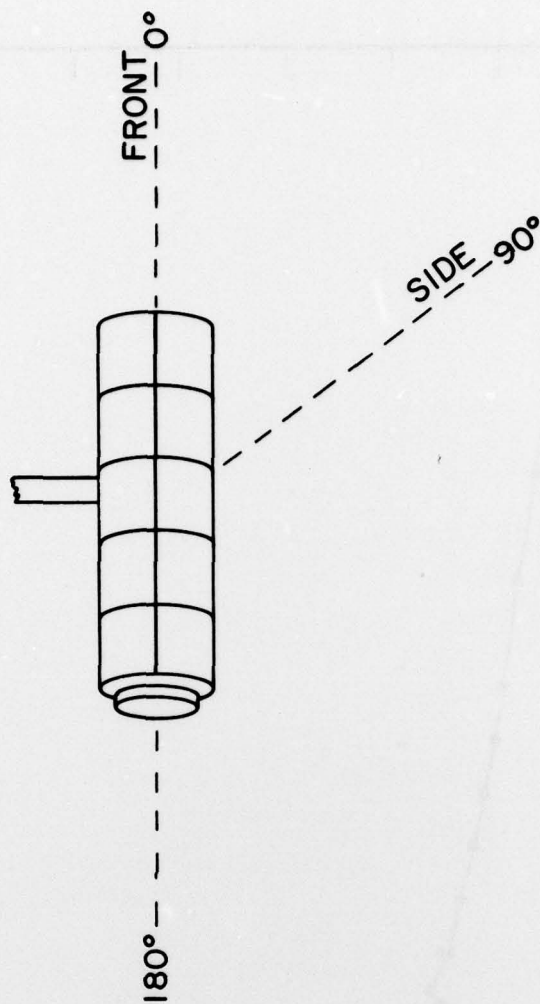
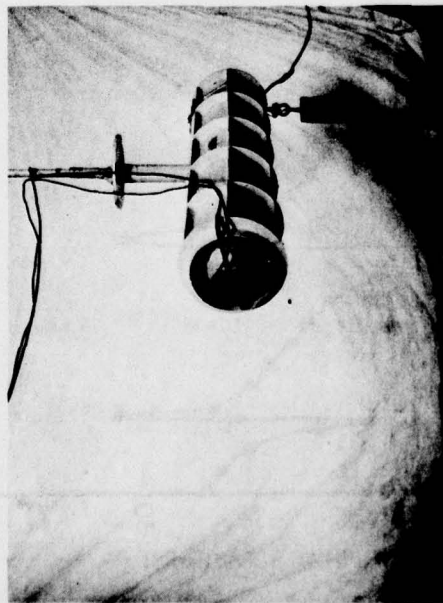


Figure C1 - Orientation of R-113 in cylindrical baffle



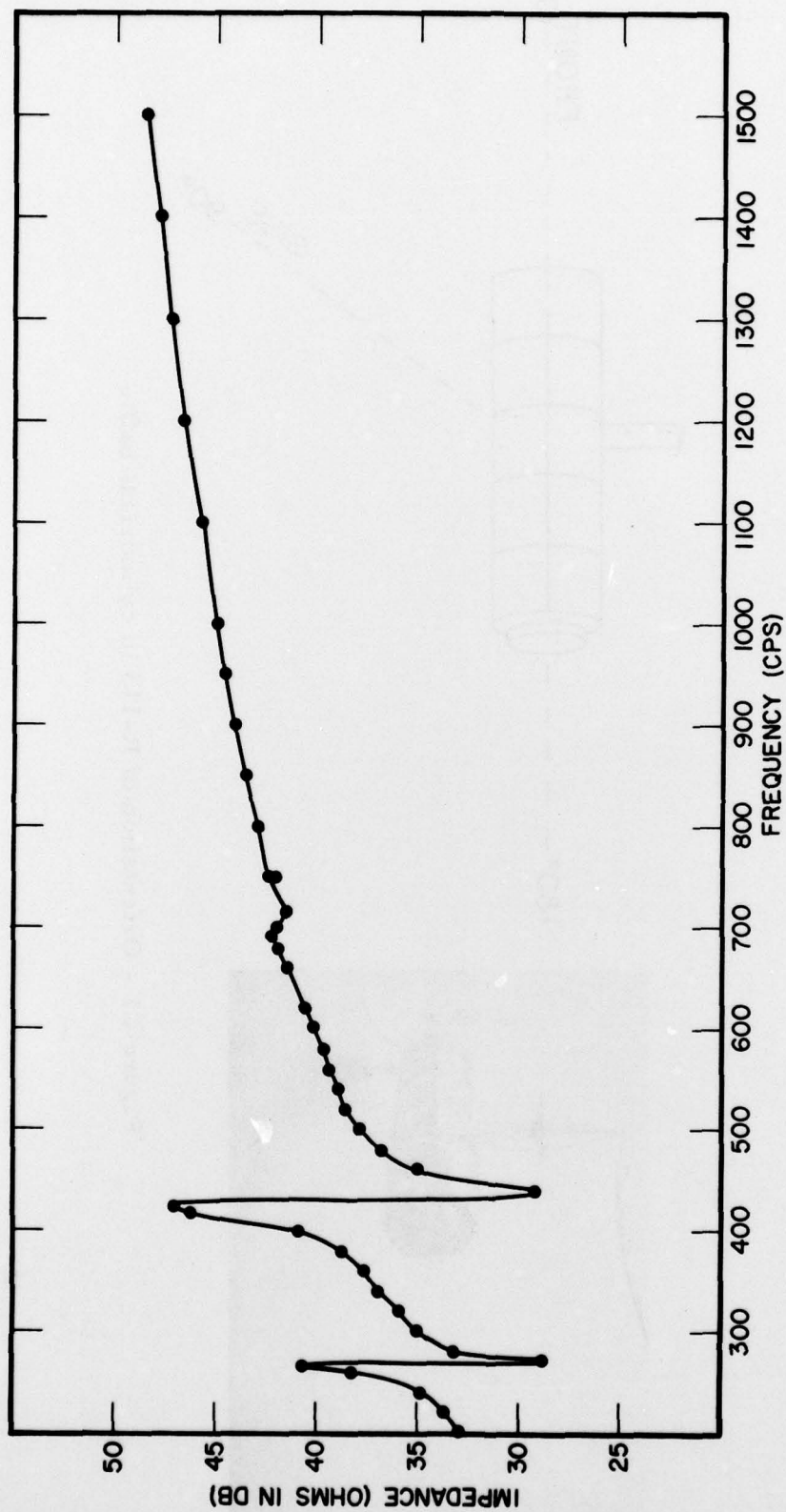


Figure C2 - Transducer impedance at current level of 0.1 rms amperes



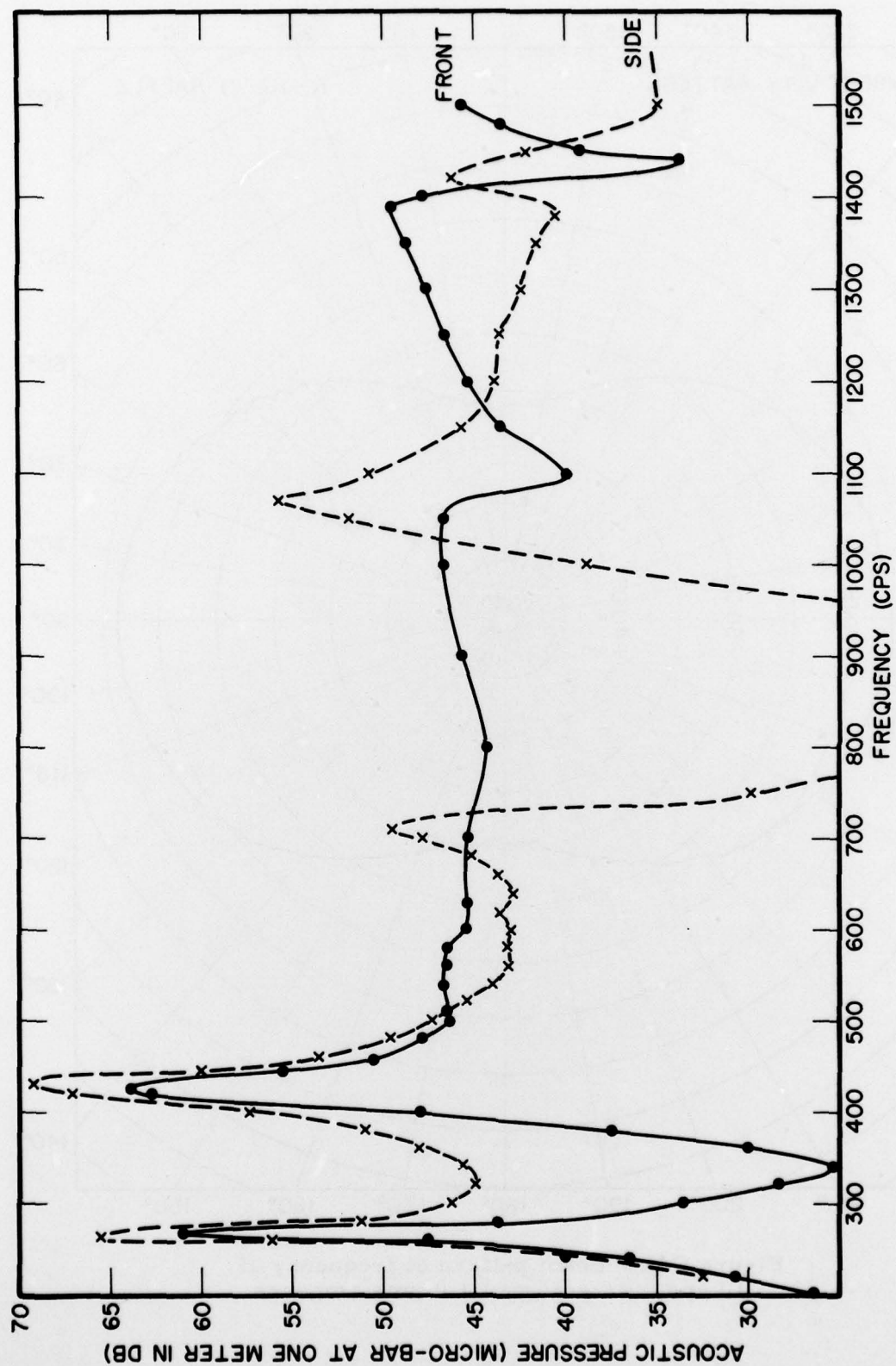


Figure C3 - Acoustic pressure in front and side direction of 0.1 rms amperes current level, transducer depth 51.7 meters, hydrophone separation 20 meters

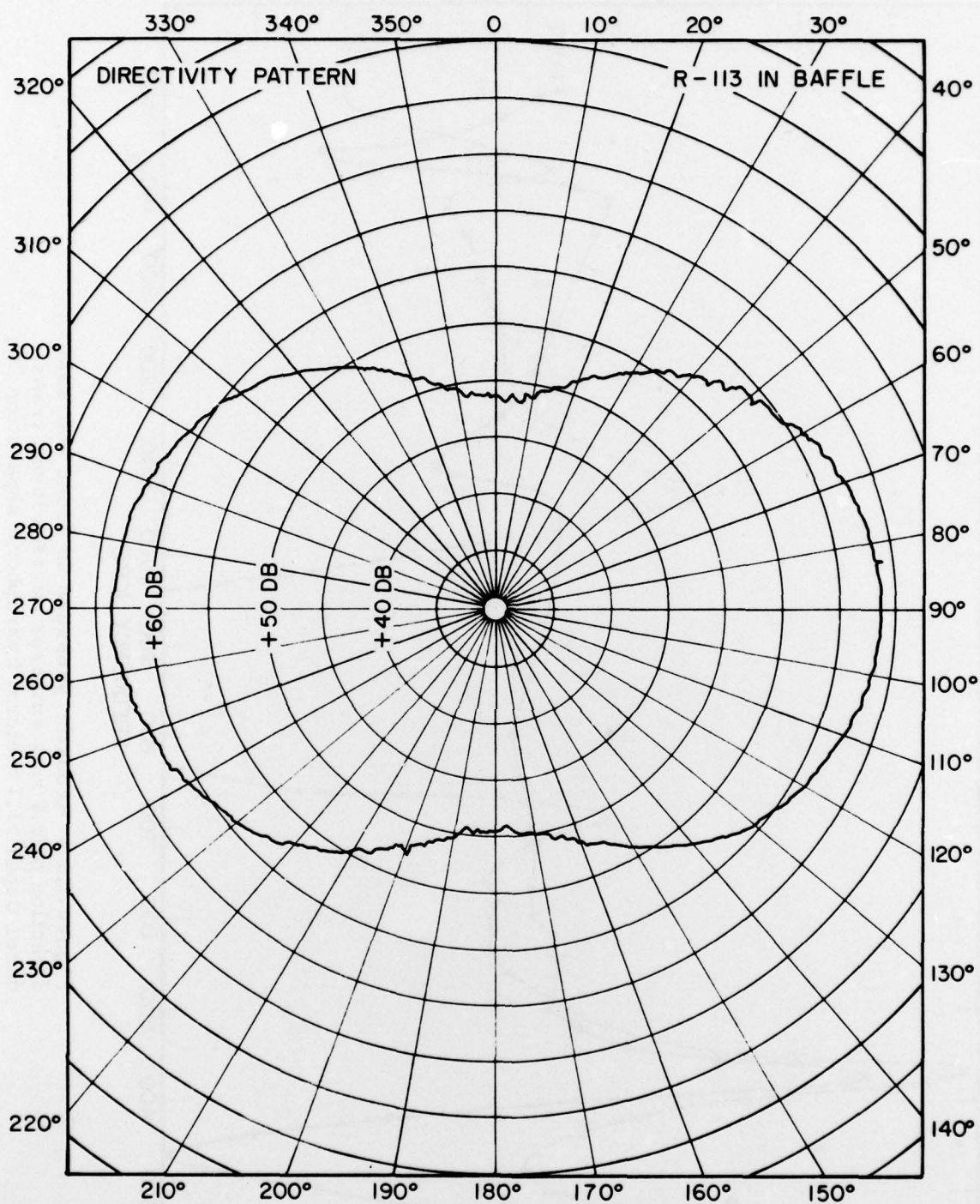


Figure C4a - Beam pattern at frequency of  
310 cps, current level 1.0 rms amperes

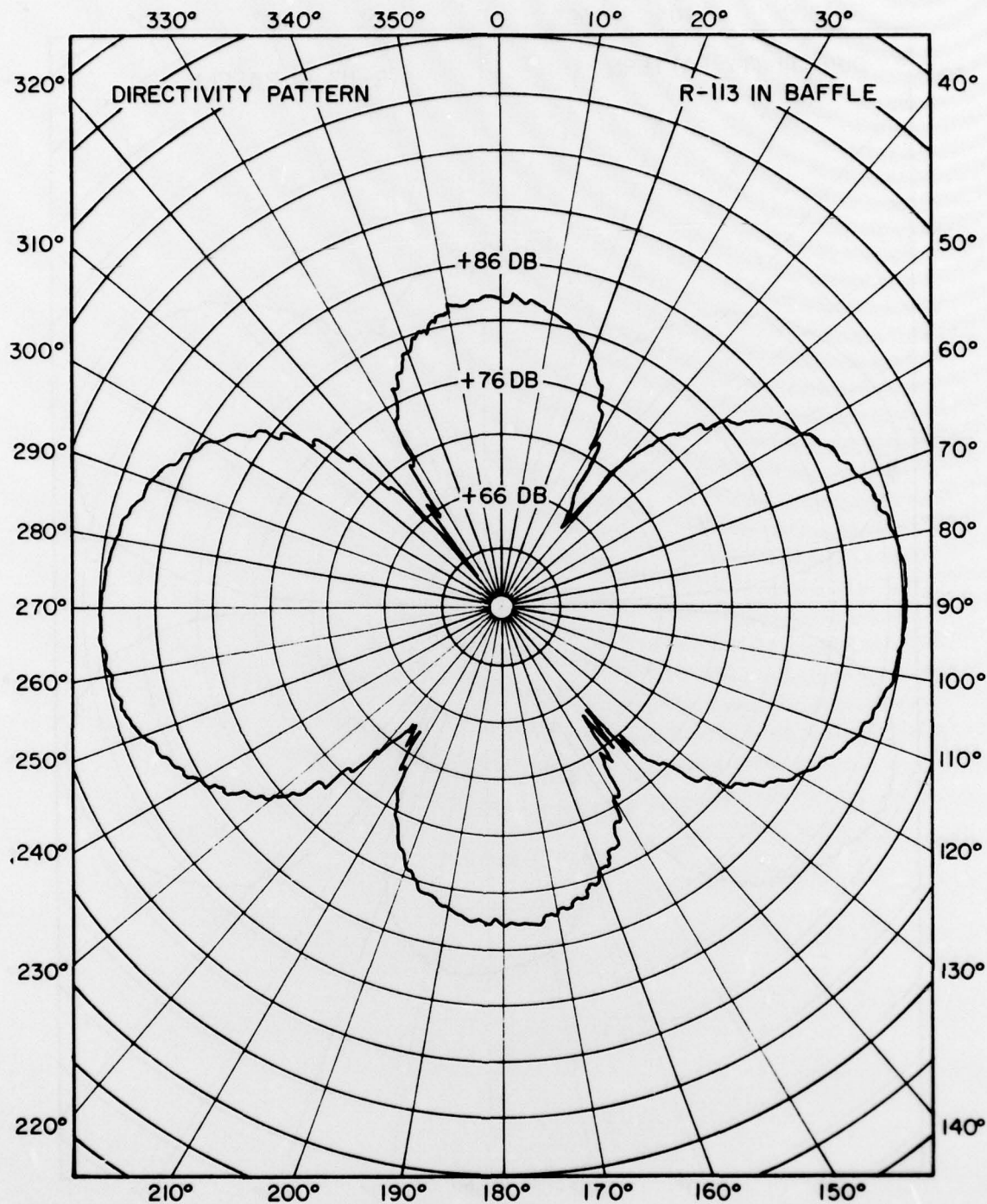


Figure C4b - Beam pattern at frequency of 413 cps.  
Current level, 1.0 rms amp; power into transducer,  
270 watts; directivity factor, 0.13; acoustic power,  
19 watts; transducer efficiency 7%.



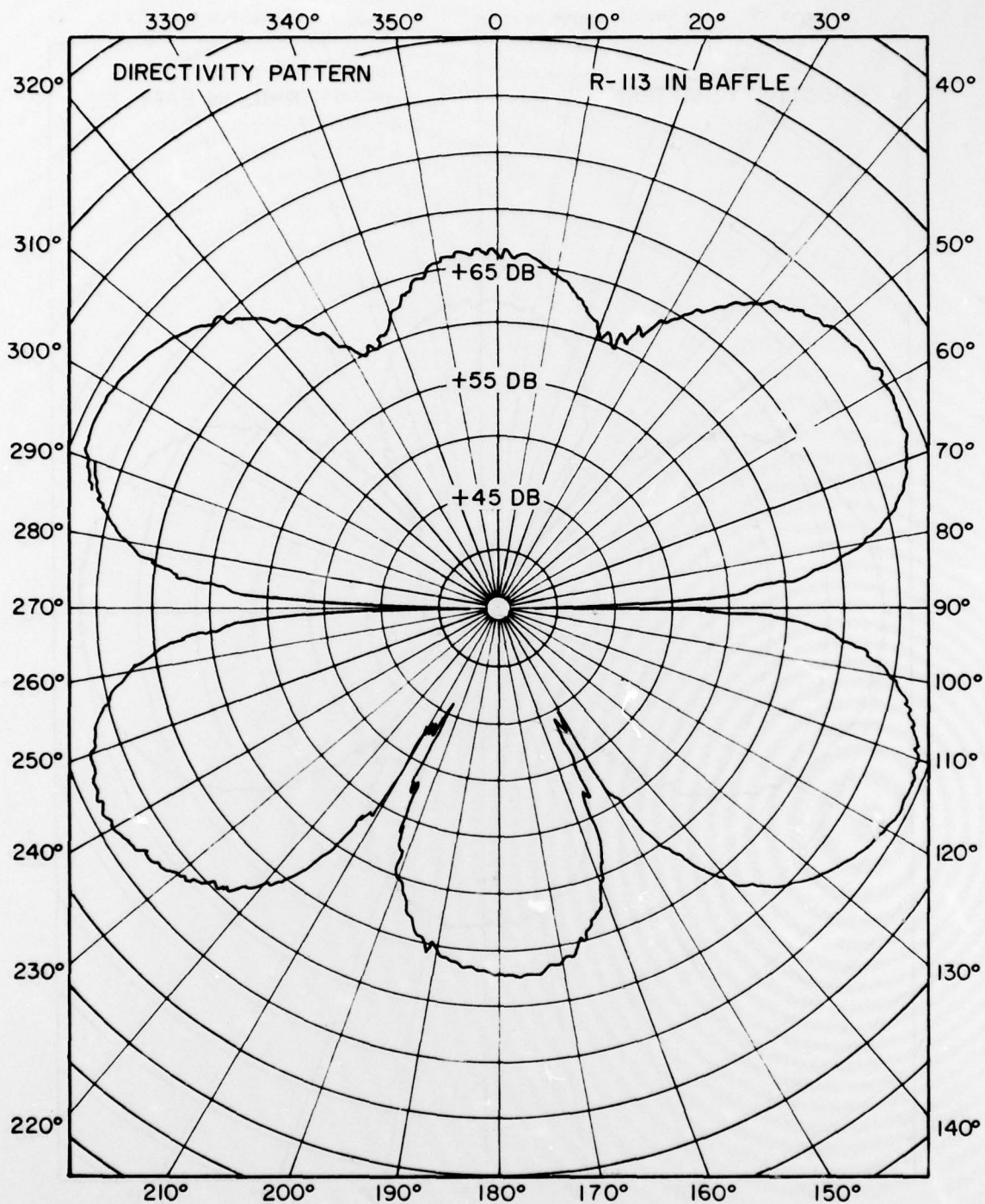


Figure C4c - Beam pattern at frequency of  
750 cps, current level 1.0 rms amperes